Meteoritics & Planetary Science 38, Nr 4, 595–626 (2003)
Abstract available online at http://meteoritics.org

Chemistry of the Calcalong Creek lunar meteorite and its relationship to lunar terranes

D. H. HILL[1*] and W. V. BOYNTON[1, 2]

[1]Lunar & Planetary Laboratory, University of Arizona, 1629 East University Blvd., Tucson, Arizona 85721–0092, USA
[2]Department of Planetary Sciences, University of Arizona, 1629 East University Blvd., Tucson, Arizona 85721–0092, USA
[*]Corresponding author. E-mail: dhill@lpl.arizona.edu

(Received 17 May 2002; revision accepted 25 April 2003)

Abstract–The Calcalong Creek lunar meteorite is a polymict breccia that contains clasts of both highlands and mare affinity. Reported here is a compilation of major, minor, and trace element data for bulk, clast, and matrix samples determined by instrumental neutron activation analysis (INAA). Petrographic information and results of electron microprobe analyses are included. The relationship of Calcalong Creek to lunar terranes, especially the Procellarum KREEP Terrane and Feldspathic Highlands Terrane, is established by the abundance of thorium, incompatible elements and their KREEP-like CI chondrite normalized pattern, FeO, and TiO_2. The highlands component is associated with Apollo 15 KREEP basalt but represents a variant of the KREEP-derived material widely found on the moon. Sources of Calcalong Creek's mare basalt components may be related to low-titanium (LT) and very low-titanium (VLT) basalts seen in other lunar meteorites but do not sample the same source. The content of some components of Calcalong Creek are found to display similarities to the composition of the South Pole-Aitken Terrane. What appear to be VLT relationships could represent new high aluminum, low titanium basalt types.

INTRODUCTION

The Calcalong Creek lunar meteorite was recovered from the Nullarbor Plain of Australia. It was the first of the "desert lunaites" recovered. Lunar meteorites are important because they represent random, and therefore, representative samples of the lunar crust (Delaney 1989) as opposed to the selective sampling of only 5% of the lunar surface during the Apollo and Luna missions. Calcalong Creek is a polymict breccia containing sub-mm clasts welded by a glassy, vesicular, matrix. In thin section, it resembles the "lunar clast-laden impact melt breccias" of the Stöffler et al. (1980) classification and shares many elemental relationships in common with other lunar polymict breccias. Our earlier work (Hill et al. 1991) showed that Calcalong Creek contains the highest abundance of incompatible elements among the known lunar meteorites.

Three lunar crustal terranes have been identified by Jolliff et al. (1999) and others, based on the remote sensing data of the Clementine and Lunar Prospector spacecraft. Distinct geochemical and petrologic provinces known as Procellarum KREEP Terrane (PKT), Feldspathic Highlands Terrane (FHT), and South Pole-Aitken Terrane (SPAT) were identified mainly by their thorium (Th) and iron oxide (FeO) abundances. Contrary to earlier ideas of "homogeneous" global stratification of the lunar crust, these terranes are thought to represent heterogeneous regions of the lunar crust and upper mantle. Haskin (1998) found a relationship between Th abundance and distance from the Imbrium basin for Lunar Prospector and Clementine data as well as samples returned from the Apollo and Luna missions. Calcalong Creek is a complex breccia that may be understood partly in terms of impact mixing of materials from these terranes.

Calcalong Creek was probably ejected from the top meter of the lunar surface where it had been exposed to cosmic rays from 2.5 million to several hundred million years (Nishiizumi et al. 1992, 1995; Swindle et al. 1995). Like the other lunar meteorites, it had a short Earth-Moon transit time of 200,000 years and is probably the only known meteorite from its impact event (Swindle et al. 1995). Calcalong Creek has one of the oldest ejection ages among lunar meteorites. Although there are interesting compositional similarities with other lunar meteorites (EET 87521/EET 96008, Y-793274, and QUE 94281), their younger ejection ages and chemical differences preclude actual pairing with Calcalong Creek (Swindle et al. 1995).

OVERVIEW OF STUDIES

Calcalong Creek studies have included petrologic examination of a 9.3 mm^2 thin section and a 75 mm^2 potted chip by Marvin and Holmberg (1992), reconnaissance microprobe studies of a 50 mm^2 thick section and 72 mm^2 thin section by Hill (this study), determination of cosmic ray exposure ages, terrestrial residence time (Nishiizumi et al. 1992; Nishiizumi et al. 1995; Swindle et al. 1995), and trace element analyses of bulk samples, clasts, and matrix (Hill et al. 1991; Hill et al. 1995). The mineralogy of the INAA clasts and the bulk rock were studied by U. Marvin in association with trace element analyses (Hill et al. 1991, 1995, this study).

EXPERIMENTAL

The University of Arizona allocation consisted of a 3.5 g piece that had been sawed from the main stone, maximizing the visible cross section. Stainless steel and diamond tools reserved for lunar samples were used to remove representative bulk chips as well as a matrix sample and individual clasts for analysis by instrumental neutron activation analysis (INAA). Handling was minimized to avoid contamination; splitting or breaking was preferred over sawing or grinding. The samples for irradiation were packaged in precleaned, high purity polyethylene vials or Suprasil quartz tubes (slide sandwich for smallest grains) and then transferred to new containers after irradiation. The meteorite was found to be very compact and consolidated, making separation of individual clasts difficult. INAA analyses of incompatible elements in 5 chips, totaling <70 mg, all exhibit <100× CI abundances with a typical KREEP pattern (Hill et al. 1991). We analyzed three bulk samples: 2,2 (38.86 mg); ,9,2,1 (18 mg); ,9,2,2 (6.2 mg); a clast-rich chip (,9,1 [3.19 mg]); and a matrix fragment (2,1 [0.34 mg]). Four clasts representing the most abundant clast lithologies were extracted from chips of Calcalong Creek. The INAA clast samples were clean splits without obvious matrix or fusion crust: clast A (150 μm [91 μg]); clast C (500 μm [350 μg]); clast D (500 μm [193 μg]); clast F (5–500 μm grains [1.16 mg total]). Splits of each clast, with some adhering matrix (except "clast A"), were removed for electron microprobe analyses. Dark clasts that comprise <5% of the specimen were not analyzed due to the difficulty of their removal. Also, there may be a sampling bias toward larger clasts.

All samples, except the largest bulk sample, were irradiated twice at the University of Arizona TRIGA reactor with neutron fluence of 2.1×10^{12} ncm^{-2} (rabbit facility) and 2.5×10^{15} ncm^{-2} (lazy susan) and at the University of Missouri Research Reactor with a neutron fluence of 1.38×10^{19} ncm^{-2} (H1 reflector). The largest bulk sample (,30) experienced TRIGA irradiation conditions of 1.26×10^{13} ncm^{-2} and 7.5×10^{15} ncm^{-2}. Counting for the short irradiation was carried out on an EG & G Ortec coaxial GeLi detector 54.6 mm in diameter, 67 mm long, at the Nuclear Engineering Department at the University of Arizona. Samples were counted twice for a live time of 200 sec at a distance of 2 cm. The Gamma-Ray Spectroscopy Lab of the Lunar & Planetary Laboratory at the University of Arizona was used in the longer irradiations. The samples were assayed on three spectrometers using several geometries as appropriate to provide <3000 cps: EG & G ORTEC HPGe (coaxial low-energy photon) detector, 51.9 mm in diameter, 20.0 mm long, 11% efficiency; EG & G ORTEC coaxial intrinsic germanium detector, 59.5 mm in diameter, 61.8 mm long 37% efficiency; PGT coaxial GeLi detector/NaI scintillator comprising our anticoincidence/coincidence, Compton suppression system, 58.4 mm in diameter, 36.5 mm long, 24% efficiency. The assay periods were typically: 1 hr to 2 days after EOB; 2 days to 1 week; 2 weeks to 4 weeks; 4–8 weeks. Each sample or split was counted at least twice per assay period. Counting times were adjusted to the count rates and decay times. They ranged from 1 hr to 12 hr. The University of Arizona microprobe studies were conducted with a Cameca SX50 electron microprobe with 15 keV accelerating voltage, 20 nA current, and 1-micron beam.

RESULTS AND DISCUSSION

General Texture and Composition

Microscopic observation of bulk pieces reveal a variety of clast types and mineral fragments as described by Marvin and Holmberg (1992). The matrix is dark and fine-grained with regions of glassy matrix. These regions appear black and "spongy" with vesicles 2–20 microns in diameter, very much like the "black breccia" lunar sample 12013 studied by Quick et al. (1977) (Fig. 1a). In thin section, the meteorite resembles the lunar clast-laden impact melt breccias of the Stöffler et al. (1980) classification. We report on our trace element survey of representative clasts as well as final INAA analyses of bulk samples. Calcalong Creek could be called a regolith breccia but has too few spherules and metal grains. Calcalong Creek is compositionally similar to crystalline impact melt breccias. Its bulk and matrix compositions (Table 1) fall within typical ranges for Al_2O_3 (16–22%) and FeO (7–12%) (Papike et al. 2000). A portion of the material in crystalline impact melt breccias was totally melted and degassed during the formation of the breccia (Papike et al. 2000). Calcalong Creek shows evidence of some melting and, perhaps, incomplete degassing. Iron sulfide, zinc sulfide, and zirconium minerals were observed by EDS on the edges of some vesicles and in nearby quenched matrix. Calcalong Creek contains a significant incompatible element component typical of polymict breccias and impact melt breccias.

The averages of all INAA experiments are presented in

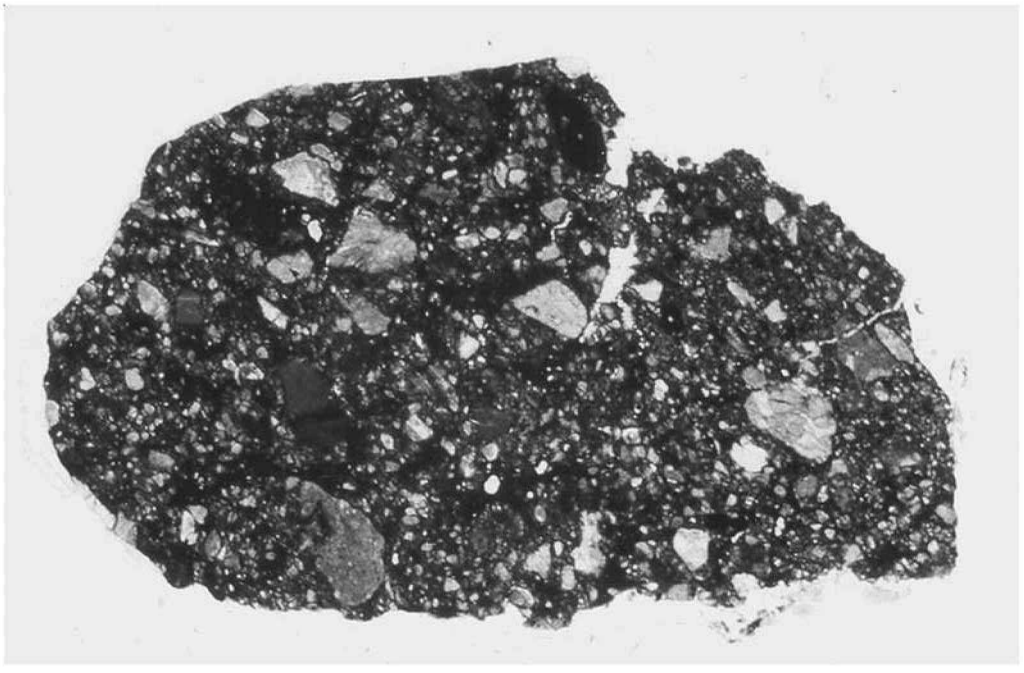

Fig. 1a. Typical microscopic view in transmitted light of Calcalong Creek, TS2, 1.1 cm across. Clasts and mineral fragments mostly composed of pyroxene and plagioclase are set in a dark, vesicular matrix. The clasts range from ~1 micron to several mm. A small-scale alignment of the largest clasts is visible in the cross section.

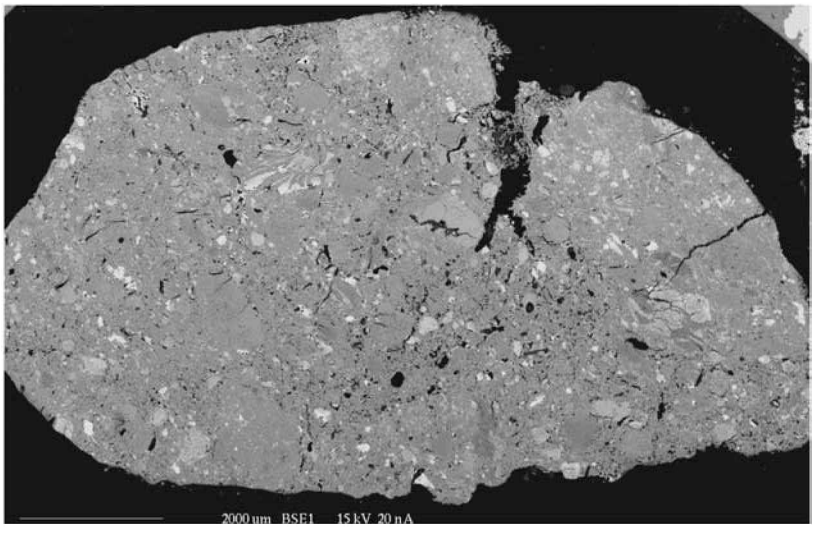

Fig. 1b. The BSE image shows plagioclase and pyroxene in a plagioclase-rich matrix. The light areas are mafic (mostly pyroxene) and the darker regions are plagioclase (anorthite). The bright grains are more Fe-rich silicates, ilmenite, and FeS.

Tables 1 and 2. Our earlier work established that Calcalong Creek is a mixture of highlands and mare materials. The bulk sample contains 0.2× the incompatible element abundance (Hill et al. 1991) compared to typical hi-K KREEP (Warren and Wasson 1979) (Fig. 2). Bulk compositions plot in the highlands field of the Ti versus Ca/Al diagram (Wood 1975) (Fig. 3) yet, Calcalong Creek just meets the CaO/Al_2O_3 >0.75 criterion (Naney et al. 1976) established for mare glasses, suggesting it is compatible with a mixture of highlands and mare components. Individual clasts plot in both the highland and mare fields of Fig. 3. Other lunar meteorites shown to contain mare material, such as replicate bulk samples of EET 87521 (Lindstrom et al. 1991; Warren and Kallemeyn 1989), also plot in both highland and mare fields. Both Calcalong Creek and Y-793274 (Lindstrom et al. 1991; Warren and Kallemeyn 1991) plot in the highlands field and near the

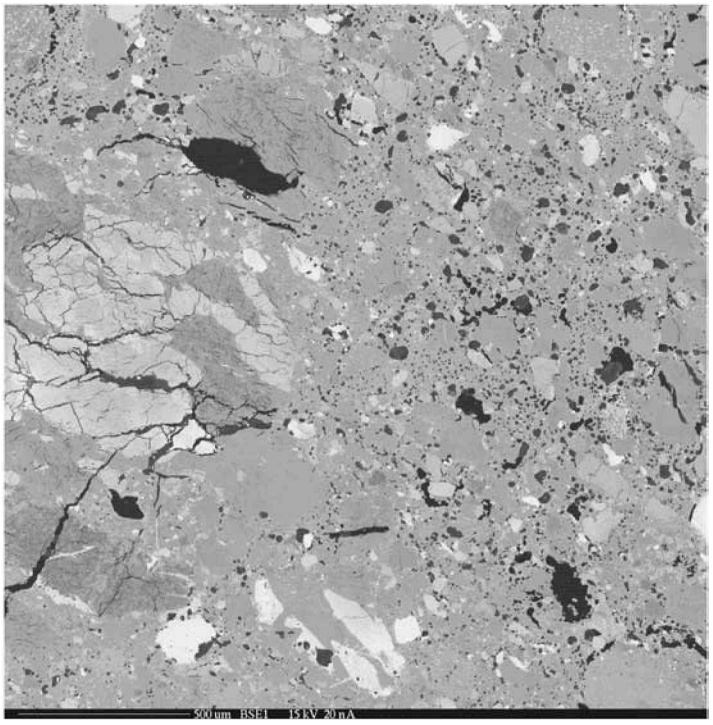

Fig. 1c. Electron microprobe BSE image of a 2 mm wide region of Calcalong Creek used for modal analysis. The bright phases are ilmenite, troilite, and Zr-minerals; the light gray phase is pyroxene and a small amount of olivine; the medium gray is plagioclase; and the darker gray is kspar and high silica clasts.

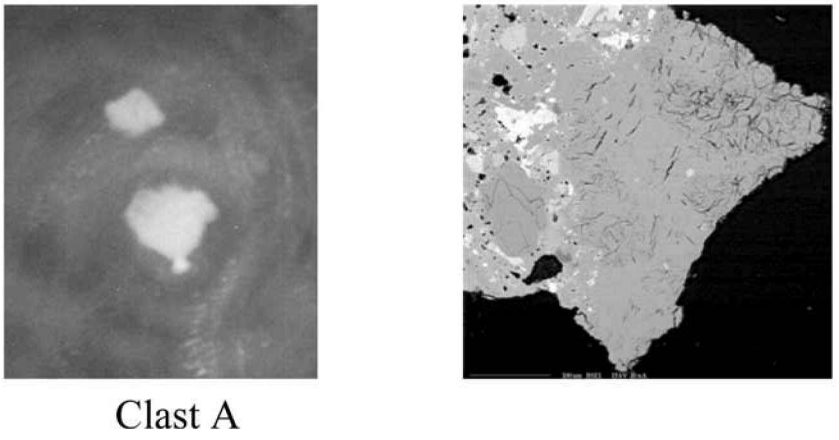

Fig. 1d. INAA sample clast A. On the left is an optical microscope view (reflected light) of the analyzed sample, which was originally ~150 microns wide. The right hand image is the BSE electron microprobe view. The light gray is plagioclase.

demarcation line defined by the polymict breccias 15558 and 79135. All three meteorites are breccias in which each chip analyzed may contain different proportions of highlands and mare components. Palme et al. (1991) identified mare and highlands samples based on their Mg and Cr contents compared to CI chondrites. On this basis, the bulk samples, clast C, and clast F are grouped with mare samples. However, other considerations indicate a significant highlands constituent.

Mineralogy

The modal analysis of Calcalong Creek was determined from a series of X-ray maps of the thin section (TS2 from UA 146, 4B) using the University of Arizona's Cameca electron microprobe. The mineral volume proportions are as follows: 26% plagioclase; 60% pyroxene; 2% olivine: 0.2% kspar; <0.2% ilmenite (includes ulvöspinel); <0.1% whitlockite (and apatite); 0.1% troilite; and 0.01% chromite. The remaining

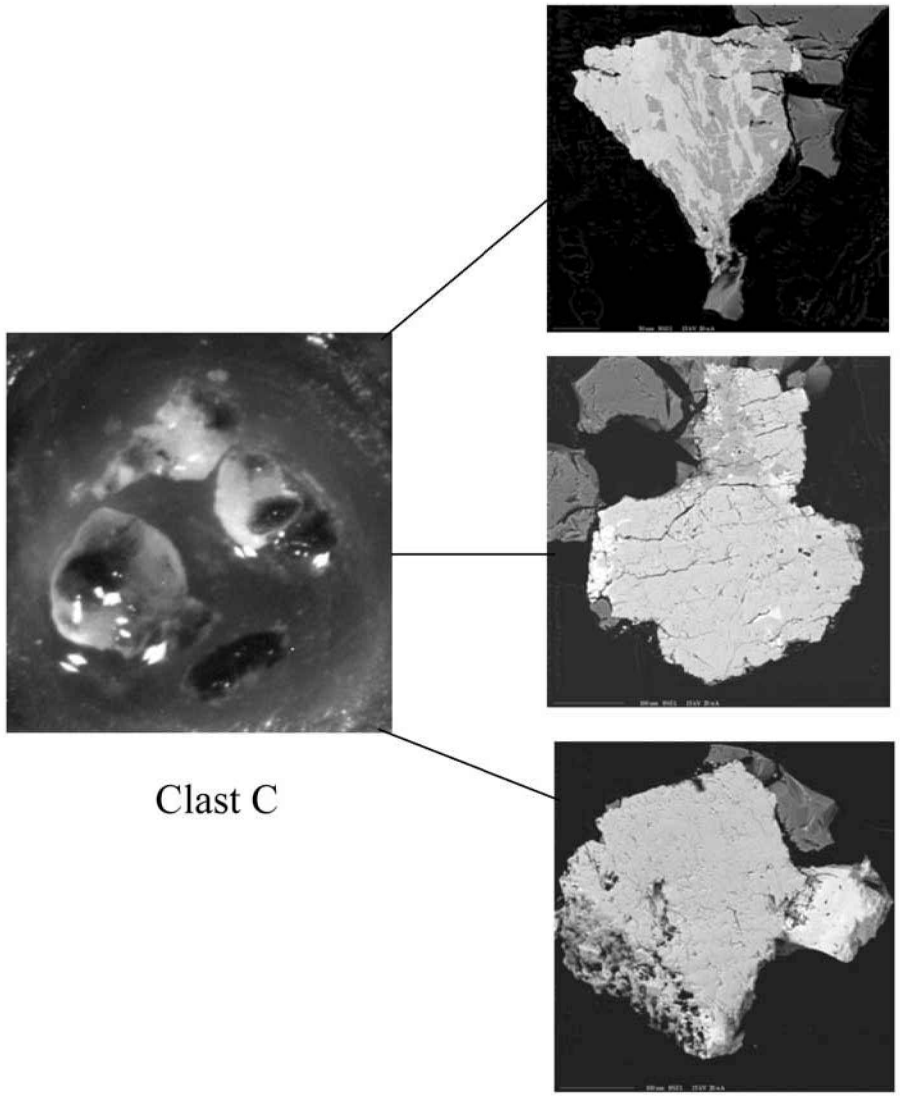

Fig 1e. INAA sample clast C. On the left is the optical microscope view (reflected light) of the analyzed sample, which was originally 500 microns wide. The right hand image is the BSE electron microprobe view. In the topmost photo, the light gray is pyroxene and the medium gray is plagioclase. The middle and bottom photos are mainly pyroxene. The brighter areas are Fe-enriched pyroxene. The attached grain in the bottom view has the same composition as the pyroxenes in the topmost grain. (The dark, angular grains adjacent to the clast are remnants of silicone oil used to affix the grain to the Suprasil slide during irradiation.)

~11% includes vesicles and less than 1% of other minerals. A relatively large pyroxene-dominated clast was prominent in each of two regions used for the modal analysis that may have affected the overall pyroxene to plagioclase ratio. Overall, clasts range from 3–4 microns to 1.5 mm set in a plagioclase-rich glass containing vesicles 2–20 microns in diameter. Some are round and others are irregular vugs. The dominant clast type is plagioclase An_{95-97}. Next in abundance is Fe-rich pyroxene. Many of the smaller pyroxene clasts are exsolved and some, but not all, exhibit shock dislocations. Representative mineral compositions for 2 thin sections are shown in Table 3.

Highlands lithologies included the most igneous-looking clast in Marvin's section, a crystalline gabbroic anorthosite with a cumulate texture (Marvin, personal communication). This clast is a ferroan anorthosite with 65% plagioclase An_{97} and 35% pyroxene. The only Mg-suite clast was large, wedge-shaped, and had a fine-grained, recrystallized texture of plagioclase An_{97} and Fe-rich olivine Fa_{91} with a groundmass of spinel troctolite. A ferroan anorthosite clast was found with 96% plagioclase An_{97} and 2 grains of clinohypersthene and olivine Fo_{61}.

Mare pyroxenes range from Mg-clinobronzites to pyroxferroites and "everything in between" (Marvin, personal communication). An iron-enriched mare basalt assemblage of ferrohedenbergite contained Al-bearing ulvöspinel rimming

ilmenite. Silica, with euhedral crystals of fayalite (Fo_{90}), is found along some pyroxene-ulvöspinel grain boundaries, along with one grain of FeS. Marvin found that their mineralogy bears strong resemblances to Luna 16 basalts and are also reminiscent of Apollo 15 mare basalts with Fe-augites, ulvöspinel, and pyroxferroite. One grain of spinel was found (chromite with MgAlTi) as well as ilmenite and ulvöspinel with 0–0.8% Cr_2O_3.

Clasts Analyzed by INAA

Three of the clasts analyzed by INAA were 100–500 μm in size (Figs. 1d–1g). They contain much lower abundances of incompatible elements (10–30 × CI) than the bulk rock, but all exhibit a typical KREEP pattern (Fig. 4). None of these clasts is considered to be pristine with respect to REE or siderophiles. The clasts analyzed in this study are representative of the types found in Calcalong Creek with the exception of Ti-rich minerals (ilmenite, ulvöspinel), which occur as small blades in basalt clasts, rounded grains in the matrix, and isolated late-stage assemblages. The clasts analyzed represent predominantly highland or mare materials but also exhibit evidence of mixing. Although each clast represents an "endpoint extremum" from which bulk compositions were derived, our sampling probably did not include all existing clasts types. Microprobe analyses of INAA samples are shown in Table 4 along with data from splits removed during the initial sample preparation.

Clast A

Clearly, many of the clasts and mineral grains in Calcalong Creek were completely melted. Clast A is one such melted particle. It is whitish to the naked eye. Microscopic inspection of the probe mount split reveals a transparent, colorless grain except for what appears to be tiny, dark, inclusions entrained in the interior and edges. These inclusions exhibit a granular and "fuzzy" appearance when slightly concentrated together. Two-thirds of the clast displays a vesicular region in which the vesicles are aligned to the interface between this region and the "clean" region. A pale green, anhedral grain exists at one edge, along with a few minute opaque grains that are part of the remaining section. These grains may be responsible for the clast's elevated Ni and Ir abundances. Clast A plots with VLT mare basalts when comparing Al_2O_3 and Sm. Its very low abundances of major and minor oxides suggest that it samples the typical high SiO_2 phase observed in the larger thin sections. If this is true, clast A contains excess Al and Fe. The INAA sample was lost during post-experiment polishing, so no direct measurements of SiO_2 exist. The incompatible element pattern seen in other Calcalong Creek materials analyzed (Fig. 4) is observed in clast A.

Clast C

Clast C is crystalline and greenish-yellow in color. This clast resembles mare pyroxenes. Trace element comparisons indicate that it extends the previously known VLT mare basalt trends. It contains about 3× the bulk Calcalong Creek abundances of Sc, Cr, and V. Taylor et al. (1978) developed a criterion for VLT composition which included: CaO/Al_2O_3 >0.75 and TiO_2 <1.1%; MgO ranges from 6–22%. Using these criteria, clast C is a VLT mare basalt ($CaO/Al_2O_3 = 2.15$; TiO_2 <0.98%; MgO = 12.1%). Melted clasts similar to clast C in composition could be the source of the relatively high "mare" elements also observed in the matrix (Sc, Cr, V, and Mg).

Clast C is a melt clast that is exotic to the predominantly highlands components of Calcalong Creek but has participated in impact mixing during lithification of the rock. Its major elemental composition retains its original imprint,

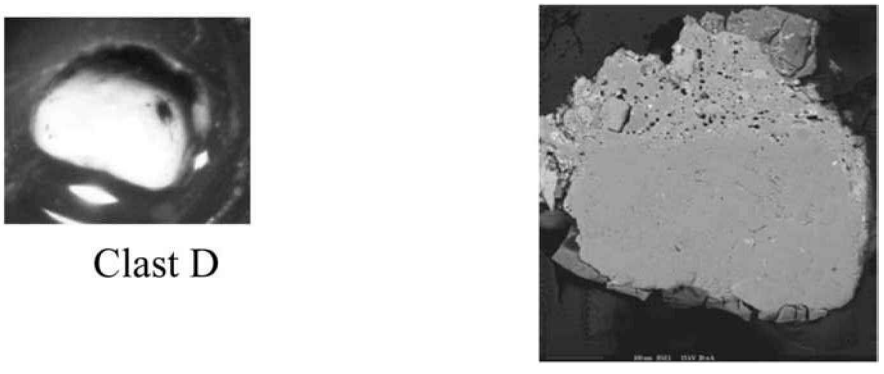

Fig. 1f. INAA sample clast D. On the left is the optical microscope view (reflected light) of the analyzed sample, which was originally 500 microns wide. The right hand image is the BSE electron microprobe view. The sample is mostly plagioclase with attached matrix that appears somewhat exaggerated in this view due to the small remnant. (The dark, angular grains adjacent to the clast are remnants of silicone oil used to affix the grain to the Suprasil slide during irradiation.)

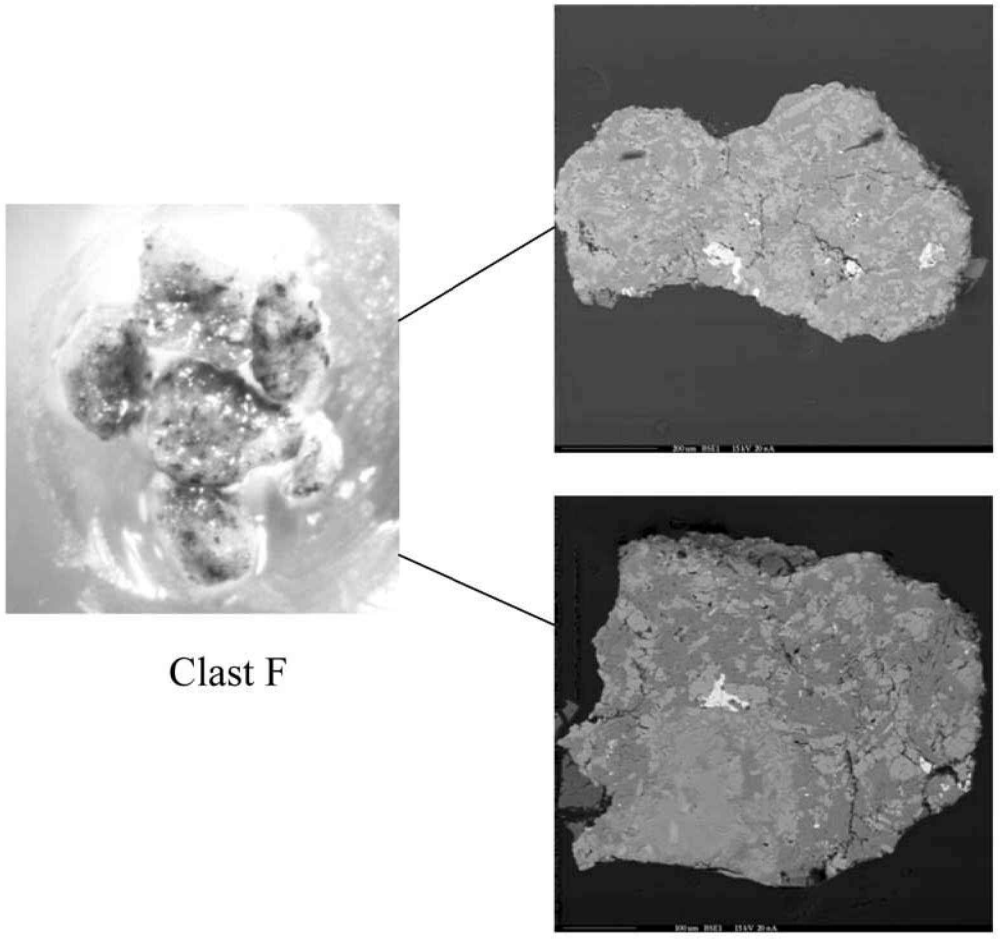

Fig. 1g. INAA sample clast F. On the left is the optical microscope view (reflected light) of the analyzed sample, which was originally >1000 microns wide. The right hand images are BSE electron microprobe views of several grains. The light gray is pyroxene and the dark gray is plagioclase. The brightest inclusions are ilmenite and FeS. (The dark, angular grains adjacent to the clast are remnants of silicone oil used to adhere the grain to the Suprasil slide during irradiation.)

but trace elements are dominated by later contamination or possible assimilation of the same KREEP-derived material that seems to pervade the rock.

Clast D

Clast D is a white clast that broke into 4 tiny grains. It is probably also related to VLT mare basalts ($CaO/Al_2O_3 = 0.88$; TiO_2 <0.4%). It plots with mare basalts for Sc/Sm versus Mn/Sm but exhibits a highlands affinity by its high Al content (Al = 14.6%). Excess Na, Eu, and Sr indicate a significant plagioclase content exists. Clast D is also probably a mixed impact melt. Although clast D exhibits enriched REE abundances, Eu anomalies are absent (Fig. 4). Perhaps, it is also an impact mixture of the REE carrier and plagioclase. Its REE pattern closely resembles that of a troctolite. However, the clast does not have high enough Mg to be a troctolite. Clast D has low Ni and high lithophiles (Sr, Rb, Th, U, K, and Ba); volatiles and other siderophiles are high relative to spinel troctolites (Taylor 1982). The INAA sample included a partial rim of adhering matrix <50 microns thick that may be the real source of the REE. Clast D also displays suspiciously high Ag (<440 ppm?). Laul et al. (1971) found Ag to be 30× higher in regolith breccias than in picritic glasses. Haskin and Warren (1991) noted that Ag is much higher in breccias than can be accounted for by meteoritic contamination. Electron dispersive spectroscopy (EDS) investigation of the INAA remnant revealed a small cluster of Ag-bearing grains with Ti, Cu, and Cr, 3 microns in diameter, welded to the clast. This, too, may not be indigenous to the clast itself.

KREEPy? Clast F

A polished mount prepared for electron microprobe analyses contains a roughly triangular remnant, 1.7 mm across, of clast F attached to a large fragment of matrix. The section was analyzed by Marvin (Hill et al. 1995), who determined the modal composition of the clast to be about

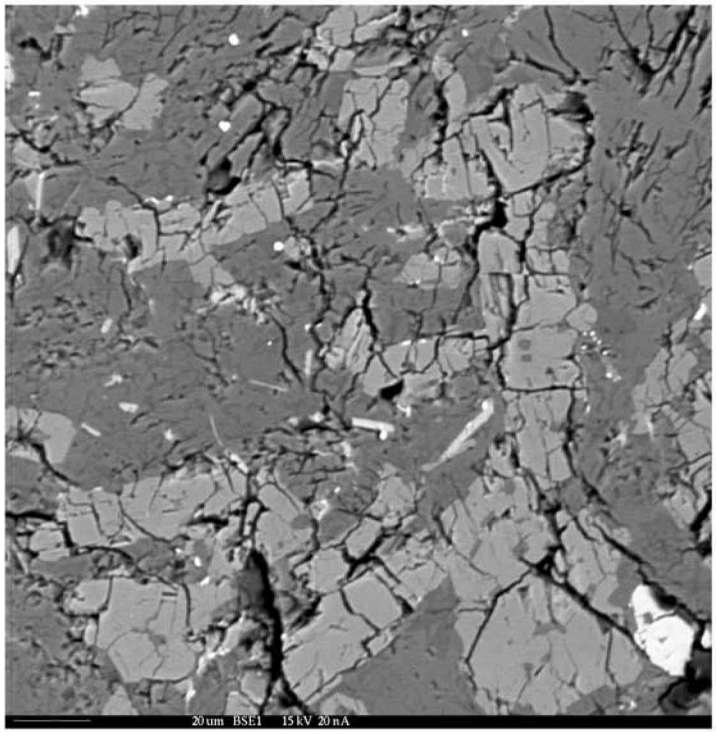

Fig. 1h. INAA sample clast F, grain F, BSE microprobe image. In addition to pyroxene and plagioclase, elongated bars and needles of phosphate minerals are present.

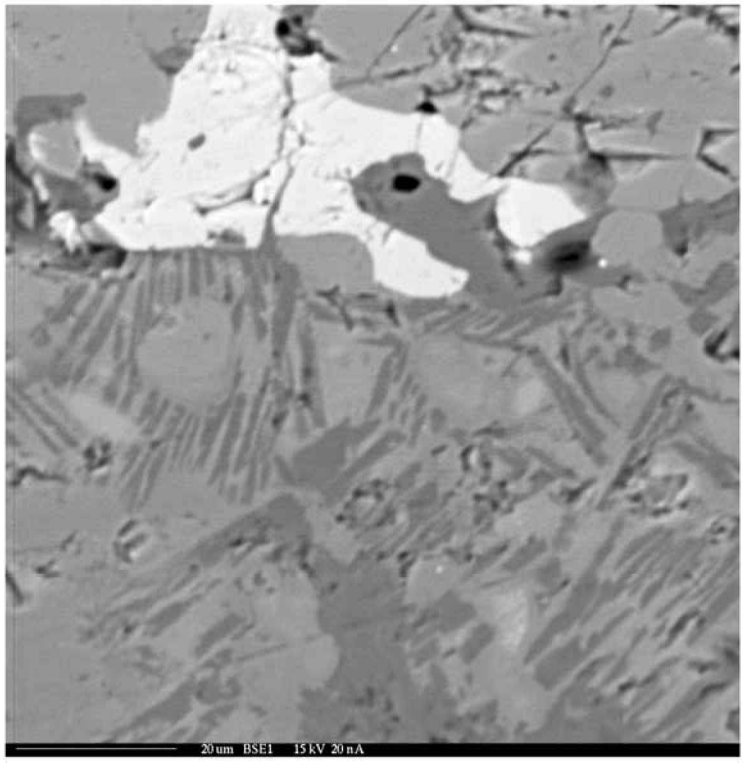

Fig. 1i. INAA sample clast F, grain F, BSE microprobe image showing a large, bright, ilmenite and "quasi-variolitic" texture of an unusual phosphorus-bearing pyroxene and plagioclase intergrowth.

Table 1. Compilation of Calcalong Creek INAA concentrations for bulk and matrix samples from all experiments.[a]

		Bulk sample ,9,2,1		Bulk sample ,9,2,2		Bulk sample ,5		Average Bulk		Bulk/clasts ,9,1		Matrix ,2,1	
		18.9 mg	s.d.	6.1 mg	s.d.	38.8 mg	s.d.		s.d.	3 mg	s.d.	0.3 mg	s.d.
Na	ppm	3590	40	3670	40	3600	40	3619	21	3450	30	3760	40
Mg	%	n.d.	n.d.	3.9	0.4	4.9	0.5	4.3	1.3	2.5	0.25	5.7	0.6
Al	%	11.2	0.3	10.72	0.16	11.4	0.19	11.02	0.12	11.61	0.14	10.46	0.14
K	ppm	2040	40	1920	40	2030	60	1986	25	1590	50	1680	140
Ca	%	9.81	0.28	9.36	0.17	9.7	0.4	9.51	0.14	10.05	0.30	9.33	0.17
Sc	ppm	22.49	0.17	21.60	0.12	17.68	0.23	21.24	0.09	15.66	0.13	24.88	0.27
Ti	ppm	4400	400	5900	500	5100	1020	5000	300	3700	400	n.d.	n.d.
V	ppm	54	5	65	5	48	5	55.3	3.0	47	5	85	14
Cr	ppm	1301	12	1146	7	1099	13	1170	5	835	8	1752	19
Mn	ppm	1133	12	1068	12	950	40	1091	8	851	9	1214	16
Fe	%	7.85	0.07	7.66	0.04	6.87	0.07	7.53	0.03	5.82	0.06	8.54	0.12
Co	ppm	25.11	0.24	23.97	0.16	26.9	0.27	24.82	0.12	19.55	0.21	28.3	0.28
Ni	ppm	273	10	159	4	202	8	180	3	129	12	151	5
Zn	ppm	n.d.	n.d.	5.68	0.28	7.2	1.2	n.d.	n.d.	4.4	1.1	5.7	0.5
Ga	ppm	n.d.	n.d.	n.d.	n.d.	4.7	0.4	4.7	0.4	2.9	0.6	7.7	2.6
As	ppm	n.d.	n.d.	0.22	0.07	0.12	0.04	n.d.	n.d.	n.d.	n.d.	0.192	0.019
Br	ppm	0.566	0.019	1.67	0.03	n.d.	n.d.	0.829	0.016	0.42	0.08	0.22	0.04
Rb	ppm	10.1	0.4	9.0	0.3	7.7	0.8	9.37	0.23	6.1	0.6	7.29	0.28
Sr	ppm	141	6	150.4	2.6	153	11	149.2	2.4	160	9	129	4
Zr	ppm	250	12	375	4	187	13	354	3	212	11	236	5
Mo	ppm	1.83	0.19	1.72	0.24	n.d.	n.d.	1.79	0.15	1.7	0.3	0.94	0.21
Cs	ppm	0.37	0.01	0.37	0.01	0.44	0.09	0.367	0.007	0.281	0.015	0.33	0.018
Ba	ppm	224	17	271	7	241	10	257	6	153	14	215	4
La	ppm	21.09	0.30	22.63	0.15	20.23	0.24	21.83	0.12	18.7	0.3	19.30	0.19
Ce	ppm	53.0	0.9	54.6	0.4	51.6	1.0	54.1	0.3	41.7	0.4	48.3	0.5
Nd	ppm	28.3	0.8	29.7	0.5	30.7	0.9	29.5	0.4	24.27	0.5	29.3	0.6
Sm	ppm	9.3	0.1	10.02	0.07	8.71	0.10	9.55	0.05	7.41	0.05	8.71	0.08
Eu	ppm	1.199	0.015	1.356	0.010	1.282	0.022	1.303	0.008	1.146	0.010	1.162	0.013
Gd	ppm	11.0	0.7	10.0	0.5	n.d.	n.d.	10.5	0.7	8.8	0.5	10.7	0.5
Tb	ppm	2.01	0.05	1.946	0.019	1.83	0.05	1.941	0.017	1.483	0.021	1.735	0.028
Dy	ppm	13.23	0.17	13.40	0.26	13.2	0.7	13.28	0.14	9.64	0.22	11.9	0.5
Ho	ppm	2.83	0.06	2.96	0.11	2.49	0.05	2.67	0.04	2.31	0.12	3.3	0.7
Tm	ppm	1.60	0.06	1.450	0.024	1.06	0.05	1.407	0.021	1.19	0.04	0.96	0.04
Yb	ppm	7.52	0.07	8.10	0.06	6.69	0.07	7.50	0.04	5.69	0.06	6.5	0.07
Lu	ppm	1.036	0.013	1.050	0.009	0.945	0.014	1.024	0.007	0.796	0.010	0.911	0.013
Hf	ppm	7.69	0.16	7.93	0.08	6.58	0.07	7.15	0.05	5.39	0.14	5.5	0.11
Ta	ppm	0.966	0.012	1.015	0.012	0.95	0.04	0.991	0.008	0.752	0.016	0.824	0.019
W	ppm	0.55	0.04	0.80	0.07	0.46	0.05	0.554	0.027	0.66	0.07	0.72	0.06
Os	ppm	n.d.	n.d.	0.4	0.08	0.16	0.05	0.2	0.01	1.2	0.4	n.d.	n.d.
Ir	ppm	0.003	0.001	0.003	0.0002	0.006	0.002	0.003	0.0002	0.004	0.0004	0.003	0.0004
Au	ppm	0.003	0.001	0.002	0.0002	0.006	0.001	0.003	0.0002	0.0059	0.0009	0.002	0.0002
Th	ppm	4.40	0.04	4.303	0.029	3.76	0.08	4.280	0.023	3.36	0.03	3.39	0.03
U	ppm	1.24	0.07	1.15	0.07	1.06	0.11	1.18	0.05	0.92	0.07	0.966	0.021
Oxide wt% (calculated from INAA)													
SiO_2		53.20		48.30		46.05		47.18		50.85		45.62	
TiO_2		0.73		0.98		0.85		0.84		0.62		n.d.	
Al_2O_3		21.17		20.26		21.55		20.83		21.94		19.77	
FeO		10.10		9.86		8.84		9.69		7.49		10.98	
MnO		0.15		0.14		0.12		0.14		0.11		0.16	
MgO		n.d.		6.47		8.12		7.11		4.15		9.45	
CaO		13.73		13.10		13.57		13.31		14.07		13.05	
Na_2O		0.48		0.49		0.49		0.49		0.47		0.51	
K_2O		0.25		0.23		0.24		0.24		0.19		0.20	
Cr_2O_3		0.19		0.17		0.16		0.17		0.12		0.26	

[a]Table of concentrations in the Calcalong Creek meteorite determined by INAA. Concentrations are in ppm except for Mg, Al, Ca, and K, which are in %. Two-sigma absolute uncertainties are listed next to each value. The oxide wt% is calculated from the INAA determination. SiO_2 is an estimate calculated by the difference of the major oxides.

52% pyroxene (pigeonites and ferropigeonites), 43% plagioclase ($An_{91–97}Or_{0.1–3.0}$), and 5% olivine ($Fa_{45–78}$). Also present are 1 grain of ilmenite and 2 of chromian pleonaste. The texture is xenomorphic granular, with pyroxenes ranging up to 750 µm, olivines to 210 µm, and plagioclases to 480 µm. Marvin saw no sign of shock damage. One large pyroxene grain is zoned, with a core of $En_{58}Fs_{30}Wo_{12}$ and a margin of $En_{40}Fs_{45}Wo_{15}$. Some olivines are zoned but most vary widely in composition from grain to grain (although they may be zoned in the 3rd dimension). Attached to one pyroxene grain is a single, small, wedge-shaped mass, 45 µm long, of silica and K-feldspar containing a 20 µm lath of whitlockite. The clast visible in this probe mount contains no other phases likely to contain REE (Marvin, personal

Table 2. Compilation of INAA concentrations for separated clasts from Calcalong Creek.[a]

		Clast A		Clast C		Clast D		Clast F	
		91 µg	s.d.	350 µg	s.d.	193 µg	s.d.	1.16 mg	s.d.
Na	ppm	1129	16	745	19	3460	70	6780	60
Mg	%	n.d.	n.d.	7.3	1.3	n.d.	n.d.	3.2	1
Al	%	3.25	0.11	2.13	0.06	14.6	0.29	7.59	0.14
K	ppm	520	50	620	60	930	130	7230	170
Ca	%	n.d.	n.d.	6.19	0.13	17.4	0.3	8.25	0.19
Sc	ppm	5.65	0.17	63.3	0.4	6.27	0.06	22.4	0.1
Ti	ppm	n.d.	n.d.	5900	1800	n.d.	n.d.	11800	1010
V	ppm	n.d.	n.d.	254	13	n.d.	n.d.	49	5
Cr	ppm	159	8	3169	28	402	4	1463	7
Mn	ppm	111.4	1.6	2170	24	290	2.9	1040	111
Fe	%	2.31	0.07	12.56	0.14	2.51	0.28	7.94	0.04
Co	ppm	10.7	0.6	45.6	0.5	8.04	0.23	17.95	0.08
Ni	ppm	520	130	68	5	44	4	221	6
Zn	ppm	82	12	3.2	1.0	3.3	0.3	4.7	0.4
Ga	ppm	n.d.	n.d.	6.7	1.8	n.d.	n.d.	14	4
As	ppm	4.3	0.3	0.762	0.018	0.165	0.022	n.d.	n.d.
Br	ppm	4.3	0.9	0.105	0.023	0.150	0.030	2.98	0.21
Rb	ppm	n.d.	n.d.	1.7	0.3	3.39	0.24	22.93	0.42
Sr	ppm	2310	134	22	4	229	5	192	6
Zr	ppm	n.d.	n.d.	72	4	46	3	1135	12
Mo	ppm	n.d.	n.d.	n.d.	n.d.	0.79	0.19	3.4	0.3
Ru	ppm	9	2.7	n.d.	n.d.	n.d.	n.d.	n.d.	n.d.
Ag	ppm	<11.6		n.d.	n.d.	<446	–	<2.5	–
Sb	ppm	3.59	0.19	n.d.	n.d.	n.d.	n.d.	0.09	0.02
Cs	ppm	n.d.	n.d.	0.14	0.01	0.171	0.027	1.116	0.012
Ba	ppm	n.d.	n.d.	79	5	92	4	744	15
La	ppm	5.2	0.4	4.39	0.04	7.19	0.07	64.3	0.4
Ce	ppm	12.2	1.7	11	0.3	18	0.4	153	1
Nd	ppm	n.d.	n.d.	7.2	1.1	11.5	1.1	88.7	1.2
Sm	ppm	1.52	0.03	2.193	0.023	3.25	0.03	27.40	0.13
Eu	ppm	0.287	0.017	0.216	0.007	1.239	0.022	2.827	0.013
Gd	ppm	n.d.	n.d.	1.8	0.5	3.5	0.5	28.5	0.4
Tb	ppm	0.77	0.19	0.499	0.012	0.67	0.016	5.608	0.028
Dy	ppm	2.28	0.29	3.46	0.21	4.27	0.19	38.3	0.7
Ho	ppm	n.d.	n.d.	0.98	0.09	1.46	0.21	7.9	0.4
Tm	ppm	n.d.	n.d.	0.331	0.019	0.418	0.028	3.27	0.04
Yb	ppm	1.17	0.18	2.2	0	2.65	0.05	20.93	0.15
Lu	ppm	0.14	0.04	0.321	0.005	0.376	0.006	3.064	0.017
Hf	ppm	1.4	0.4	1.44	0.07	2.01	0.03	31.34	0.16
Ta	ppm	n.d.	n.d.	0.209	0.018	0.397	0.023	3.300	0.023
W	ppm	n.d.	n.d.	0.231	0.020	0.55	0.11	2.3	0.3
Os	ppm	n.d.	n.d.	n.d.	n.d.	n.d.	n.d.	0.79	0.06
Ir	ppm	0.048	0.008	0.003	0.0007	0.53	0.11	0.004	0.0004
Au	ppm	n.d.	n.d.	0.0005	0.0001	0.0381	0.0005	0.0053	0.0005
Th	ppm	1.04	0.22	1.116	0.023	2.07	0.04	12.14	0.08
U	ppm	0.9	0.27	0.333	0.016	0.76	0.03	3.34	0.11
Oxide wt% (calculated from INAA)									
SiO_2		90.64		58.12		44.12		54.48	
TiO_2		n.d.		0.98		n.d.		1.97	
Al_2O_3		6.14		4.03		27.59		14.34	
FeO		2.97		16.17		3.23		10.77	
MnO		0.01		0.28		0.04		0.13	
MgO		n.d.		12.10		n.d.		5.31	
CaO		n.d.		8.66		24.37		11.54	
Na_2O		0.15		0.10		0.47		0.91	
K_2O		0.06		0.07		0.11		0.87	
Cr_2O_3		0.02		0.46		0.06		0.21	

[a]Table of concentrations of representative clasts separated from the Calcalong Creek meteorite determined by INAA. Concentrations are in ppm except for Mg, Al, Ca, K, which are in %. Two-sigma absolute uncertainties are listed next to each value. The oxide wt% is calculated from the INAA determination. SiO_2 is an estimate calculated by the difference of the major oxides.

Table 3a. Representative mineral compositions in Calcalong Creek.

	Plagioclase				High-Fe plagioclase				K-spar			Pyroxenes											
												<5% CaO		5–10% CaO		10–20% CaO		<5% CaO		5–10% CaO		10–25% CaO	
	TS2 (UA)		,10 (Marvin)		TS2 (UA)		,10 (Marvin)		TS2 (UA)			TS2 (UA)		TS2 (UA)		TS2 (UA)		,10 (Marvin)		,10 (Marvin)		,10 (Marvin)	
	ave	s.d.	ave	s.d.	ave	s.d.	ave	s.d.	ave	s.d.		ave	s.d.	ave	s.d.	ave	s.d.	ave	s.d.	ave	s.d.	ave	s.d.
SiO_2	44.52	1.93	43.04	0.89	45.56	1.41	42.85	2.67	71.23	5.88		53.23	1.68	50.31	2.74	49.61	1.45	50.92	0.06	48.96	0.82	47.47	2.18
TiO_2	0.06	0.06	0.04	0.06	0.83	1.38	0.73	1.08	0.38	0.21		0.56	0.24	0.77	0.47	0.53	0.28	0.50	0.42	0.34	0.16	1.04	0.73
Al_2O_3	34.54	1.68	34.20	0.93	26.15	3.46	24.28	5.19	14.08	3.60		2.16	1.76	7.19	5.82	1.59	0.44	0.58	0.50	1.17	0.27	7.41	7.25
FeO	0.68	0.48	0.43	0.28	5.62	2.19	6.00	3.32	3.40	4.94		14.31	5.87	20.98	10.19	19.83	7.44	20.86	1.54	23.67	2.09	13.00	3.76
MnO	0.02	0.02	0.04	0.04	0.08	0.03	0.08	0.06	0.04	0.07		0.23	0.10	0.31	0.16	0.34	0.07	0.29	0.02	0.42	0.05	0.23	0.11
MgO	0.27	0.32	0.20	0.22	4.80	2.85	7.26	4.42	0.90	1.98		26.02	5.23	11.25	5.69	12.31	4.41	29.65	7.42	14.60	2.38	11.69	1.97
CaO	18.38	1.14	19.23	0.58	14.81	1.73	14.80	2.09	1.94	1.23		2.50	1.29	7.32	1.58	13.95	2.70	1.12	0.91	7.54	1.41	15.56	3.94
Na_2O	0.66	0.53	0.52	0.18	0.67	0.19	0.37	0.12	0.71	0.51		0.03	0.02	0.22	0.21	0.04	0.02	0.10	0.10	0.11	0.06	0.26	0.19
K_2O	0.07	0.06	0.06	0.05	0.33	0.46	0.12	0.12	6.82	2.33		0.01	0.01	0.57	1.11	0.01	0.01	0.02	0.02	0.01	0.02	0.09	0.10
Cr_2O_3	0.01	0.01	0.01	0.02	0.09	0.07	0.11	0.08	0.02	0.03		0.48	0.08	0.23	0.18	0.52	0.27	0.18	0.10	0.35	0.14	0.35	0.20
P_2O_5	0.03	0.02	0.33	0.06	0.17	0.15	0.24	0.10	0.08	0.06		0.01	0.01	0.13	0.17	0.02	0.02	0.20	0.04	0.21	0.08	0.32	0.09
NiO	0.01	0.01	0.04	0.04	0.02	0.02	0.02	0.02	0.02	0.02		0.00	0.00	0.02	0.02	0.02	0.02	0.01	0.01	0.05	0.05	0.04	0.05
SO_3	n.a.	n.a.	0.01	0.01	n.a.	n.a.	0.03	0.02	n.a.	n.a.		n.a.	n.a.	n.a.	n.a.	n.a.	n.a.	0.00	0.00	0.01	0.01	0.02	0.03
BaO	n.a.	n.a.	0.09	0.06	n.a.	n.a.	0.05	0.06	n.a.	n.a.		n.a.	n.a.	n.a.	n.a.	n.a.	n.a.	0.03	0.00	0.07	0.06	0.06	0.07
Total	99.24	0.86	98.25	0.73	99.13	0.92	97.71	1.35	99.61	1.26		99.54	0.50	99.30	1.19	98.77	0.61	97.20	0.09	97.48	0.86	97.54	0.39
N	39		20		45		27		5			8		13		13		2		10		11	
an	0.94	0.05	0.96	0.02	0.90	0.05	0.96	0.01	0.19	0.13	wo	0.23	0.10	0.51	0.23	0.34	0.14	0.02	0.02	0.17	0.03	0.23	0.10
or	0.00	0.00	0.01	0.00	0.02	0.03	0.01	0.01	0.71	0.13	en	0.72	0.12	0.49	0.23	0.36	0.12	0.70	0.05	0.45	0.06	en	0.72
ab	0.06	0.05	0.05	0.02	0.07	0.02	0.05	0.02	0.10	0.05	fs	0.05	0.03	0.73	0.20	0.30	0.05	0.27	0.03	0.39	0.04	fs	0.05

Table 3b. Representative mineral compositions in Calcalong Creek.

	Olivines								Phosphates									
			Low-Cal		High-Ca		High-Al		whitlockite		apatite		P-rich silicate	silica-rich		K-enriched silicate		
	TS2 (UA)		,10 (Marvin		,10 (Marvin		TS2 (UA)		TS2 (UA)		TS2 (UA)		TS2 (UA)	TS2 (UA)		TS2 (UA)		
	ave	s.d.	ave	s.d.	ave	s.d.	ave	s.d.	ave	s.d.	ave	s.d.			s.d.	ave	s.d.	
SiO_2	39.94	1.21	39.11	0.27	35.38	4.06	41.67	2.62	3.43	2.72	1.15	0.05	45.39	95.18	1.85	22.95	1.33	
TiO2	0.06	0.03	0.03	0.02	0.31	0.37	0.93	0.65	0.13	0.09	0.08	0.05	1.45	0.25	0.10	31.71	0.23	
Al_2O_3	0.19	0.21	0.04	0.02	3.62	5.68	15.18	5.14	0.69	0.71	0.42	0.24	25.72	0.68	0.21	13.77	0.94	
FeO	13.82	5.89	10.61	1.69	31.82	17.34	16.00	5.21	2.50	0.76	1.04	0.03	4.82	1.12	1.52	23.42	1.32	
MnO	0.16	0.07	0.10	0.02	0.35	0.21	0.17	0.03	0.03	0.03	0.04	0.01	0.09	0.01	0.01	0.22	0.04	
MgO	45.70	5.01	48.06	1.49	23.08	10.21	17.72	8.18	2.81	2.52	0.25	0.12	2.3	0.05	0.04	2.13	0.44	
CaO	0.21	0.11	0.08	0.02	2.64	3.17	7.88	2.86	43.41	4.88	53.16	0.18	14.91	0.32	0.42	5.78	1.09	
Na_2O	0.01	0.01	0.02	0.02	0.19	0.08	0.41	0.13	0.06	0.02	0.06	0.00	0.9	0.08	0.04	0.40	0.04	
K_2O	0.01	0.01	0.00	0.01	0.04	0.05	0.22	0.15	0.04	0.03	0.01	0.01	0.29	0.18	0.11	0.67	0.50	
Cr_2O_3	0.08	0.04	0.05	0.02	0.15	0.07	0.10	0.06	0.02	0.01	0.02	0.02	0.08	0.05	0.07	0.54	0.28	
P2O5	0.03	0.04	0.05	0.03	0.28	0.12	0.28	0.13	39.16	3.20	39.02	0.19	41.21	0.01	0.01	0.06	0.02	
NiO	0.01	0.02	0.00	0.00	0.05	0.06	0.01	0.01	0.00	0.01	0.02	0.00	0	0.01	0.01	0.02	0.02	
SO_3	n.a.	n.a.	0.01	0.01	0.01	0.01	n.a.	n.a.	n.a.	n.a.	n.a.	n.a.	0.17	n.a.	n.a.	n.a.	n.a.	
BaO	n.a.	n.a.	0.07	0.04	0.08	0.06	n.a.	n.a.	n.a.	n.a.	n.a.	n.a.	0	n.a.	n.a.	n.a.	n.a.	
Total	100.24	0.48	98.25	0.12	97.99	1.03	100.56	1.53	92.27	2.45	95.26	0.20	96.42	97.93	0.52	101.67	1.12	
N	5		5		4		6		6		2		1	4		2		
fa	0.16	0.07	0.89	0.02	0.57	0.24	0.57	0.24										
fo	0.84	0.07	0.11	0.02	0.43	0.24	0.43	0.24										

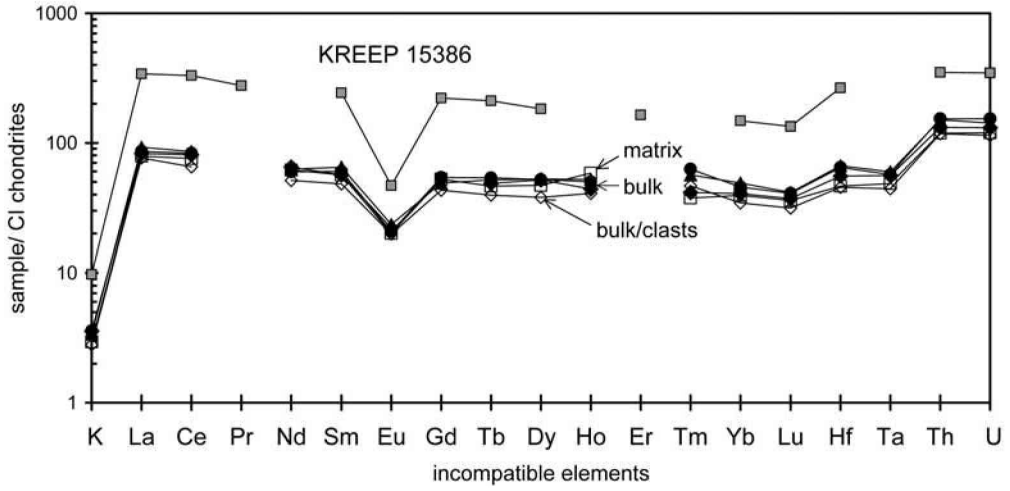

Fig. 2. Incompatible-element abundances relative to CI chondrites for bulk samples of Calcalong Creek. Hi-K KREEP (Apollo 15 sample 15386) data are from Warren and Wasson (1979). The matrix is almost indistinguishable from the bulk samples. Although the matrix appeared to be clast free during sample preparation, it contains clast fragments of 1–5 microns that must be similar to the larger clast population.

communication). Microprobe EDS analysis of two INAA grains ("B" and "F") reveals both REE-bearing and REE-poor phosphates in the form of 10–20 μm laths and oval-shaped apatite grains that are heterogeneously distributed between the grains studied (Fig. 1g). Grain F includes a region with an unusual P-bearing silicate (pyroxene?) intergrown with plagioclase in a "quasi-variolitic" texture (Fig. 1h; Table 4).

Clast F exhibits basaltic composition and its incompatible lithophiles are quite similar to the medium-K Fra Mauro basalt 15386 (med-K KREEP) (Rhodes and Hubbard 1973). Notable exceptions are excess siderophiles Ni, Ir, and Au, which could be due to meteoritic contamination or which may be indigenous to the sample (see section on Meteoritic Contamination). According to the limits adopted by Warren and Kallemeyn (1989), clast F falls on the boundary between low-Ti and very low-Ti basalts (Ti = 11800 ppm), is considered to be a high-Al mare basalt (Al = 7.6%) and high-K basalt (K = 7300 ppm). Clast F is an incompatible-element-rich VLT basalt clast. It exhibits a high CaO/Al_2O_3 ratio (0.80), indicating mare tendency, and plots near Wood's (1975) line of demarcation between mare and highland components (Fig. 3). However, clast F also exhibits a highland refractory signature (Fig. 5).

Individual grains comprising the INAA sample were separated and counted at long decay times in the high flux experiment. Although there is some scatter in the data, most grains exhibit abundances within a factor of 2 of the long-lived REE when compared to CI chondrites (Fig. 6). Therefore, the REE (incompatible elements) are relatively homogeneously distributed throughout the clast F sample (but not in large whitlockite phases or interstitial K-feldspar glass) (Hill et al. 1995). Upon closer inspection, the INAA grains exhibit a heterogeneous distribution of 20 micron long laths and needle-shaped, Ce-bearing (REE) whitlockites. However, the ratio of the highest to lowest concentration (grains 14E and 14C) of the six grains for Eu, Hf, and Th is 1.7×, and for Zr is 1.6×, and yet, Sc, an element that is correlated with REE, is fairly constant from grain to grain (Table 5). Some variation in Ca exists, which also suggests different abundances of whitlockite and mafic minerals. Siderophiles Ni, Ir, and Au also display some variability among the grains.

FORMATION OF THE MATRIX

Calcalong Creek is a small specimen, so the distinction between "wide scale" melt matrix production as in an impact melt sheet versus shock melting of regolith fines is not clear. An impact glass is expected to be homogeneous, without many clasts, unless it had been injected into an already mixed regolith (Hörz and Cintala 1997). Some patches of glass contain small mineral fragments, 1–10 microns across, and give an agglutinous appearance. However, the matrix glass does not contain many "reduced" Fe metal globules, making an agglutinate label less appropriate. Also, the edges and margins of some, but not all, clasts show evidence of some interaction with the melt and some possible degassing. Some volatile elements (Zn, S) appear to be present in and near vesicles, which indicates that some outgassing may have occurred.

Feldspar and mesostasis experience comminution preferentially over pyroxene and olivine (Korotev 1976; Papike et al. 1981; Laul et al. 1987; Hörz and Cintala 1997). They also participate preferentially in shock melting of lunar soils. This process results in the enrichment of feldspars in a shocked melt over the bulk composition of the host soil. Although the glassy matrix of Calcalong Creek is predominantly feldspathic, bulk INAA analyses show that it is also enriched relative to the bulk composition by 1.1–1.2× for

Table 4a. Microprobe analyses of INAA samples.

	Plagioclase clast A probe split[a]		clast C		clast D		clast D matrix coating		clast F grain B		clast F grain F	clast F probe split[a]		INAA matrix		Fe-rich		Na-rich
	ave	s.d.	ave	s.d.	ave	s.d.	ave	s.d.	ave	s.d.		ave	s.d.	ave	s.d.	ave	s.d.	
SiO_2	43.86	0.37	46.15	0.28	44.08	0.34	46.64	1.77	46.15	1.09	47.37	45.40	0.99	44.57	0.81	46.98	2.69	54.95
TiO2	0.09	0.38	0.12	0.16	0.01	0.01	0.28	0.20	0.06	0.04	0.12	0.02	0.02	0.05	0.04	1.03	1.88	0.02
Al_2O_3	36.50	0.29	33.51	1.49	36.91	0.28	27.65	7.93	34.10	0.48	34.68	32.92	0.71	36.06	1.02	24.15	6.41	28.75
FeO	0.23	0.18	1.71	1.37	0.14	0.03	5.12	5.24	0.48	0.13	0.28	0.91	0.12	0.59	0.41	6.83	3.72	0.53
MnO	0.01	0.01	0.02	0.02	0.01	0.01	0.05	0.07	0.01	0.01	0.03	0.01	0.01	0.01	0.01	0.10	0.07	0.03
MgO	0.07	0.12	0.17	0.12	0.02	0.01	3.28	3.72	0.12	0.11	0.01	0.21	0.08	0.23	0.44	4.57	2.87	0.03
CaO	19.42	0.18	18.03	0.61	19.57	0.12	14.28	4.27	17.35	0.53	17.66	18.12	0.64	19.14	0.62	14.89	1.98	11.41
Na_2O	0.38	0.02	0.76	0.18	0.39	0.03	0.86	0.39	1.37	0.42	1.00	0.66	0.14	0.51	0.26	0.57	0.15	4.48
K_2O	0.01	0.01	0.11	0.02	0.01	0.01	0.44	0.36	0.25	0.20	0.37	0.11	0.11	0.05	0.04	0.30	0.18	0.11
Cr_2O_3	0.01	0.01	0.01	0.02	0.02	0.02	0.08	0.08	0.02	0.03	0.00	0.02	0.01	0.01	0.02	0.13	0.13	0.04
P_2O_5	0.03	0.02	0.07	0.02	0.05	0.02	0.12	0.06	0.06	0.04	0.03	0.02	0.02	0.05	0.03	0.30	0.40	0.03
NiO	0.01	0.01	0.00	0.00	0.02	0.02	0.01	0.01	0.01	0.01	0.00	0.01	0.01	0.01	0.01	0.01	0.02	0.03
ZrO_2	0.01	0.01	0.00	0.00	0.00	0.00	1.03	2.16	0.00	0.00	0.02	n.a.	n.a.	0.00	0.01	0.02	0.05	0.04
Ce_2O_3	0.02	0.05	0.01	0.01	0.01	0.01	0.01	0.01	0.03	0.02	0.04	n.a.	n.a.	0.02	0.02	0.01	0.02	0.03
BaO	0.01	0.01	0.02	0.01	0.03	0.03	0.05	0.03	0.08	0.02	0.07	n.a.	n.a.	0.02	0.02	0.03	0.05	0.11
SO_4	n.a.	n.a.	n.a.	n.a.	n.a.	n.a.	n.a.	n.a.	n.a.	n.a.	n.a.	0.01	0.01	n.a.	n.a.	n.a.	n.a.	n.a.
Total	100.64	0.63	100.71	0.57	101.25	0.40	99.92	1.13	100.09	0.79	101.68	98.39	0.27	101.31	0.89	99.93	1.73	100.59
N	23		6		8		7		5		1	4		25		17		1

[a]Microprobe split (Marvin and Holmberg [1992] data).

Table 4b. Microprobe analyses of INAA samples.

	Pyroxenes clast C		clast D	clast F grain B		clast F grain F		grain F augite		microprobe split[a]				INAA matrix mafic <5% CaO		mafic 5-10 % CaO		mafic 10-20% CaO		INAA matrix banded pyx	
	ave	s.d.		ave	s.d.	ave	s.d.	ave	s.d.	ave	s.d.	ave	s.d.	ave	s.d.	ave	s.d.	ave	s.d.	lt. phase	dk. phase
SiO_2	48.62	1.68	52.71	50.76	0.90	51.40	0.09	48.01	1.25	44.64	6.93	51.25	0.71	51.36	1.17	49.80	1.99	50.02	1.57	50.04	49.53
TiO_2	0.60	0.27	0.50	1.07	0.53	0.96	0.37	0.95	0.15	0.53	0.35	0.20	0.06	0.52	0.36	0.50	0.39	0.76	0.33	1.09	1.13
Al_2O_3	3.94	3.47	1.02	1.01	0.33	0.79	0.13	17.77	2.70	0.76	0.48	1.13	0.34	1.12	0.42	2.29	2.26	2.82	3.54	1.62	1.71
FeO	28.16	6.25	12.77	22.28	0.69	22.35	0.68	7.88	1.74	35.29	6.31	24.00	2.27	23.51	3.41	26.37	4.88	21.87	7.88	19.08	17.52
MnO	0.42	0.07	0.27	0.35	0.03	0.36	0.02	0.14	0.02	0.43	0.04	0.40	0.03	0.40	0.03	0.42	0.06	0.35	0.08	0.37	0.33
MgO	9.58	4.64	13.82	19.56	0.49	19.83	0.41	5.77	1.04	11.91	7.86	17.42	1.97	19.07	3.18	12.98	2.82	10.73	3.84	12.51	12.22
CaO	8.28	2.56	19.92	4.04	0.31	4.02	0.27	14.60	1.35	7.37	5.35	5.87	1.41	3.67	1.17	7.41	1.33	13.48	3.48	14.49	15.71
Na_2O	0.08	0.09	0.04	0.04	0.01	0.04	0.01	0.89	0.36	0.01	0.01	0.01	0.01	0.04	0.02	0.05	0.05	0.07	0.07	0.11	0.09
K_2O	0.05	0.07	0.00	0.01	0.01	0.02	0.01	0.75	0.09	0.00	0.01	0.00	0.00	0.05	0.06	0.04	0.05	0.03	0.04	0	0
Cr_2O_3	0.13	0.33	0.31	0.47	0.10	0.40	0.02	0.13	0.05	0.11	0.10	0.46	0.17	0.26	0.23	0.33	0.17	0.34	0.20	0.51	0.6
P_2O_5	0.07	0.06	0.07	0.03	0.01	0.02	0.02	4.02	1.27	0.04	0.04	0.02	0.02	0.10	0.16	0.04	0.05	0.04	0.05	0.01	0.03
NiO	0.02	0.03	0.04	0.00	0.01	0.02	0.01	0.04	0.08	0.00	0.01	0.02	0.02	0.03	0.03	0.02	0.02	0.02	0.03	0	0
ZrO_2	0.01	0.01	0.00	0.03	0.02	0.01	0.00	0.11	0.03	n.a.	n.a.	n.a.	n.a.	0.03	0.07	0.00	0.00	0.01	0.02	0.01	0
Ce_2O_3	0.00	0.00	0.00	0.00	0.00	0.00	0.03	0.02	0.02	n.a.	n.a.	n.a.	n.a.	0.00	0.00	0.25	0.99	0.01	0.02	0	0
BaO	0.01	0.01	0.00	0.01	0.01	0.01	0.01	0.07	0.04	n.a.	n.a.	n.a.	n.a.	0.02	0.02	0.02	0.02	0.01	0.02	0.01	0.01
SO_4	n.a.	n.a.	n.a.	n.a.	n.a.	n.a.	n.a.	n.a.	n.a.	0.01	0.01	0.01	0.01	n.a.	n.a.	n.a.	n.a.	n.a.	n.a.	n.a.	n.a.
Total	99.98	1.16	101.46	99.66	1.15	100.23	0.60	101.12	0.94	101.10	1.18	100.75	0.74	100.14	0.39	100.51	1.29	100.57	1.18	99.88	98.89
N	21		1	5		4		4		4		17		6		8		6		1	1

[a]Microprobe split (Marvin and Holmberg [1992] data).

Table 4c. Microprobe analyses of INAA samples.

	Olivines																							
				INAA matrix					high silica			Phosphates	Ilmenite	Chromites		P-rich silicate								
				High-Mg ves				Low-				clast F	clast F			clast F								
	clast C	clast F[a]		mtx		clasts in mtx		Mg clast				grain F	grain B		clast F[a]		clast F[a]			grain B	grain F			
		ave	s.d.	ave	s.d.	ave	s.d.	in mtx	ave	s.d.	INAA	apatite	matrix			ave	s.d.						ave	s.d.
SiO_2	42.90	31.73	0.22	39.00	0.15	35.89	0.71	31.39	96.49	1.25		0.95	0.54	0.13	0.10	0.13	0.02	54.00	48.46	1.05	46.65	42.45	45.63	9.86
TiO_2	0.61	0.02	0.02	0.05	0.01	0.05	0.01	0.10	0.16	0.03		0.09	0.04	53.24	53.04	0.83	0.04	0.45	0.88	0.09	1.15	0.68	0.36	0.14
Al_2O_3	3.76	0.02	0.01	0.02	0.01	0.03	0.00	0.02	1.24	0.85		0.15	0.02	0.08	0.13	11.7	0.18	16.74	18.52	2.75	15.50	0.91	9.18	1.75
FeO	9.75	57.57	3.83	19.64	0.25	34.89	4.60	61.42	0.30	0.11		0.71	0.87	40.11	44.48	35.28	0.57	0.76	7.91	2.13	7.80	20.16	2.07	1.63
MnO	0.11	0.55	0.07	0.22	0.01	0.34	0.11	0.88	0.02	0.02		0.04	0.05	0.35	0.3	0.29	0	0.00	0.13	0.03	0.15	0.3	0.00	0.00
MgO	43.30	10.86	1.85	42.14	0.07	29.36	2.55	4.78	0.13	0.21		0.17	0	4.38	1.2	2.14	0.14	0.67	5.56	1.17	6.39	16.25	1.03	0.23
CaO	1.76	0.39	0.06	0.16	0.04	0.17	0.07	0.41	0.42	0.34		54.46	55.01	0.17	0.4	0.04	0.02	12.98	13.99	0.70	16.43	10.95	17.38	3.28
Na_2O	0.12	0.01	0.01	0.02	0.01	0.00	0.00	0.00	0.11	0.08		0.04	0.04	0	0	0.02	0.02	0.97	0.89	0.44	0.86	0.09	0.38	0.16
K_2O	0.17	0.00	0.01	0.00	0.00	0.00	0.00	0.00	0.18	0.05		0.02	0	0.00	0	0	0	2.43	0.71	0.01	0.88	0.07	1.88	0.04
Cr_2O_3	0.03	0.03	0.02	0.07	0.03	0.01	0.01	0.00	0.00	0.01		0.02	0	0.57	0.13	48.26	0.65	0.01	0.11	0.04	0.18	0.23	0.02	0.00
P_2O_5	0.05	0.00	0.00	0.02	0.01	0.05	0.04	0.05	0.00	0.01		40.77	41.39	0.02	0	0.01	0.01	8.73	3.44	0.68	5.73	8.58	19.15	1.24
NiO	0.02	0.02	0.01	0.05	0.00	0.01	0.01	0.00	0.02	0.03		0.02	0	0.00	0.04	0	0	0.01	0.05	0.01	0.00	0	0.03	0.04
ZrO_2	0	n.a.	n.a.	0.01	0.01	0.01	0.01	0.03	0.00	0.01		0.28	0.31	0.00	n.a.	n.a.	n.a.	0.26	0.08	0.08	0.19	0	0.11	0.07
Ce^2O^3	0	n.a.	n.a.	0.00	0.00	0.00	0.00	0.00	0.01	0.01		0.25	0.16	0.00	n.a.	n.a.	n.a.	0.65	0.02	0.03	0.00	0.62	1.13	0.13
BaO	0.02	n.a.	n.a.	0.01	0.01	0.03	0.02	0.00	0.01	0.01		0	0.02	0.16	n.a.	n.a.	n.a.	0.09	0.06	0.04	0.10	0.01	0.07	0.04
SO^2	n.a.	0.02	0.01	n.a.	n.a.	n.a.	n.a.	n.a.	n.a.	n.a.		n.a.	n.a.	n.a.	0	0	0	n.a.	n.a.	n.a.	n.a.	n.a.	n.a.	n.a.
Total	102.59	101.21	2.32	101.38	0.05	100.83	2.74	99.08	99.11	0.50		97.98	98.45	99.21	100.21	98.72	0.03	98.76	100.82	0.90	102.00	101.29	98.41	1.68
#	1	3		2		2		1	3			1	1	1	1	2		1	3		1	1	2	

[a]Microprobe split (Marvin and Holmberg [1992] data).

Fe, Co, Mn, Sc; 1.3× for Mg and As; and 1.5–1.6× for V, Cr, and Ga but not Ni. Calcalong Creek is depleted by about 0.85× for most other elements: K, Rb, Sr, REE, Hf, Ta, Th, and U and more so for Au, Zr (0.7×), Mo (0.5×), and Br (0.3×). Although the glassy regions resemble agglutinates, they contain few metal globules and, as mentioned above, are not necessarily enriched in a feldspathic component with respect to the bulk composition. Microprobe analyses by Marvin (personal communication) of 10-micron spots indicate that there are definite mafic and feldspathic areas within the vesicular glass, i.e., the glass is not homogeneous on a small scale (<<100 microns) but may be more so on a scale of millimeters. The glass, possibly, was formed during lithification in a process suggested by Schaal and Hörz (1980), Simon et al. (1986), and others in which fine soil particles are melted by frictional heating during a compressive phase of a shock wave and later cool to form glass.

WHAT SHOCK, PRESSURE, AND THERMAL REGIMES WERE EXPERIENCED?

Marvin and Holmberg (1992) suggested that Calcalong Creek experienced low shock levels and at least 2 impact events, based on the appearance of the matrix and the welding of dissimilar materials. Calcalong Creek is a well-mixed sample that could have experienced typical impact gardening from small impacts in a regolith setting. One of the thin sections (TS2, 4a) exhibits an alignment of 4 relatively large clasts (~<1 mm), as well as other smaller ones, near the center of the section, along its longest axis. The clasts have different compositions and textures, indicating that they were entrained in the melted matrix as opposed to undergoing cataclasis during a small-scale impact. The alignment visible in other sections is less obvious. Rare schlieren glass suggestive of agglutinate production is present in some areas. Large scale crater deposits are known to produce mixtures of "primary" and local materials deposited at ambient temperatures, while impact melts and hot impact deposits are confined to crater interiors (Simonds et al. 1976). Exsolution lamellae, 2–5 microns wide, in many pyroxenes indicate that slow cooling occurred, perhaps insulated by a thick ejecta blanket before lithification. Few clasts have sharp boundaries with the vesicular matrix and almost always contain vesicles at their edges and, sometimes their interiors. Some clasts appear to retain some of their original textures and were not completely melted. These clasts tend to be larger (1 mm range) with basaltic compositions and textures. These samples exhibited the same frothy, vesicular matrix and some flow banding. Maskelynite is observed in some clasts but is formed over such a wide pressure range that it does not indicate a unique pressure regime. Shock-induced fractures are present in large pyroxenes and displaced exsolution lamellae are observed in some smaller grains.

The maximum pressure experienced during lithification

of the rock was probably in the realm of 25 GPa as suggested by Hawke and Head (1979) to be typical of primary Imbrium ejecta. The highest pressure experienced by some clasts before lithification of the rock could have been as high as 27–50 GPa since the texture of Calcalong Creek is consistent with that of experimental samples produced by See et al. (2001). Marvin and Holmberg (1992) proposed that heating from a shock pulse may have melted some phases in Calcalong Creek. The presence of some more volatile trace elements also indicates that Calcalong Creek was spared from extended high temperatures. Ostertag et al. (1986) attributed different shock stages in clasts and matrix of the lunar meteorite Y-791197 to their being shocked before inclusion in the glassy matrix. Similar to Y-791197, the presence of intergranular melt but scarcity of maskelynite points to overall pressures between 10–20 GPa. Studies by Schaal et al. (1979) found that shock pressures required to produce glasses in loose regolith are almost a factor of 2 lower than in solid, crystalline rock (45.8 GPa versus >80 GPa). Shocked and annealed clasts from impacts of various distances were incorporated into loose regolith that produced the intergranular melt of Calcalong Creek during shock lithification. That molten impact ejecta was injected into already mixed, loose regolith is also possible. No doubt exists that multiple processes occurred.

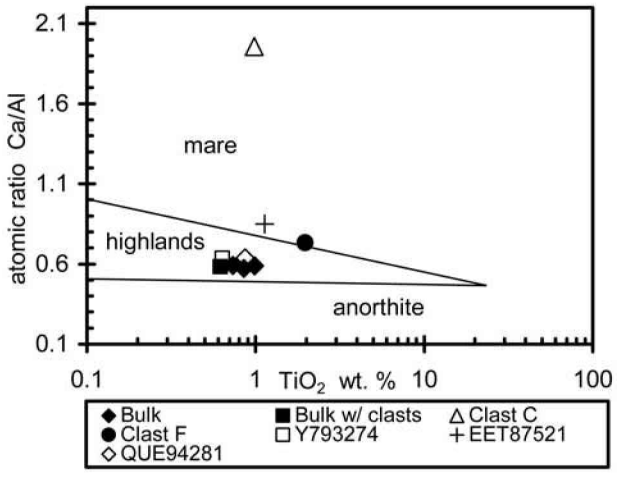

Fig. 3. Wood's mare/highlands diagram shows the provenance of Calcalong Creek and other lunar meteorites for each region, based on atomic Ca/Al and wt% TiO_2. The division between mare and highlands fields is defined by lunar polymict breccias 15558 and 79135. Clast C is the only INAA sample with a clear mare origin. The rest plot in the highlands field. Individual clasts in polymict breccias may plot in different fields depending on their provenance. The data for Y-793274 is from Lindstrom et al. (1991) for and EET 85721 is from Warren and Kallemeyn (1991).

SIDEROPHILE ELEMENTS AND POSSIBLE METEORITIC CONTAMINATION

Siderophile elements in bulk Calcalong Creek (Au, Ir, Ni, and Co) are consistent with minimal overall meteoritic contamination (0.5–1%, Hill et al. 1991; Korotev 1999). Individual impact clasts may contain a higher fraction. A few rare grains of iron-nickel metal, 1–100 microns across, were found in the matrix and also inside impact melts. Unfortunately, most were too small to analyze quantitatively. One kamacite grain with a composition of $Fe_{92}Ni_7Co_1$ is similar to the iron-nickel-bolide estimate ($Fe_{94}Ni_6Co_{0.4}$) that Korotev used in his mixing models of mafic impact breccias (Korotev 1999). The matrix sample analyzed, the most likely carrier of any potential meteoritic projectile, contains about the same (or slightly less) Ni (151 ppm), Au (0.002 ppm), and Ir (0.003 ppm) as the bulk rock but more Co (28.3 ppm). James (1996) estimated that the indigenous Ni in the lunar crust ranges from ~16 ppm lunar-wide to 50 ppm at the Apollo 16 site. Although bulk Calcalong Creek contains 3–10× the Apollo 16 abundances (159–273 ppm), we argue that the nonchondritic ratios suggest that Ni, especially, comes from lunar materials. Indeed, Ni is found to be higher in volcanic glasses (>100 ppm, Delano 1986) than in mare basalts for similar TiO_2 abundances. All of the samples of Calcalong Creek analyzed in this study contain >100 ppm Ni, except the VLT-mare clast C (68 ppm) and clast D (44 ppm). Clast F displays a very high Ni content (221 ppm) relative to normal KREEP basalt abundances (~10 ppm) but is within the range of other mafic impact melt breccias (<335 ppm) (Jolliff 1999). Warren et al. (1989) suggested that high nickel content alone is not necessarily the best indication of meteoritic contamination in lunar rocks, so other siderophile ratios were investigated.

In some pristine highlands samples, the Ni/Ir ratio normalized to CI chondrites is up to 2 orders of magnitude higher than for Calcalong Creek and other lunar meteorites; 50–100 (Ryder and Norman 1978) compared with 0.004–3.9 for Calcalong Creek, 0.01 for Dhofar 26 (Warren et al. 2001) and 1.2 for QUE 94281 (this lab). Calcalong Creek bulk samples, although higher in Ni, are found to be consistent with contamination by carbonaceous or enstatite chondrites with respect to their Co/Au and Ni/Ir ratios. Clast C and, to some degree, EET 85721 exhibit a near chondritic Ni/Ir ratio but also a large Co/Au ratio not associated with chondrites or iron nickel groups. Elevated Ni could also be a signature from the mare source. The Co/Au ratio is, possibly, an analytical artifact due to low abundances of Au and a small sample size. However, this is usually manifested by anomalously high concentrations. The chondrite-normalized ratios of Co and Ni/Ir for clast C, a mare basalt, show a clear similarity to bulk samples of Y-793274, EET 87521, and QUE 94281 (Fig. 7). This provides additional evidence that clast C shares the imprint of a common class of impactor or, more likely, is related to the VLT mare components of these lunar meteorites. Clast D is even lower than Dhofar 26, a sample already identified as enigmatic for siderophile content (Warren et al. 2001). With respect to other siderophile

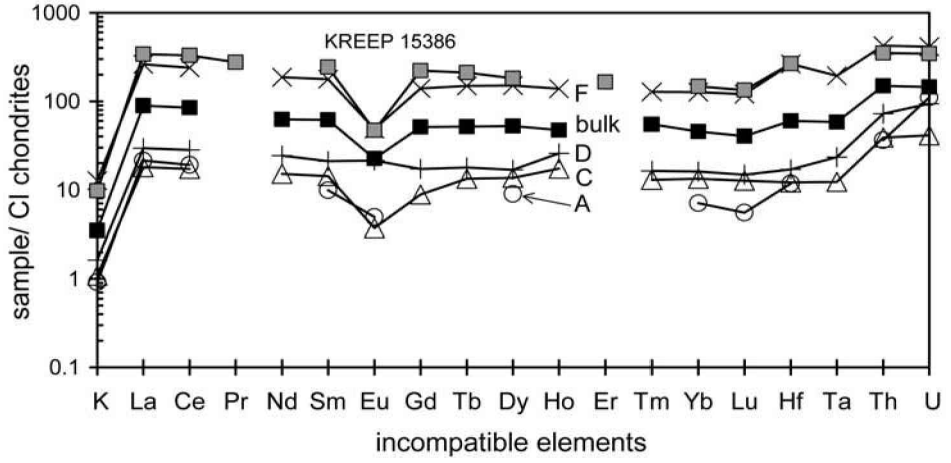

Fig. 4. Incompatible element abundances relative to CI chondrites for clasts of Calcalong Creek analyzed by INAA. All clasts display a KREEP-like rare earth pattern. Clast D exhibits excess europium, suggesting that it may contain a higher plagioclase component than the other clasts. Matrix contamination may be responsible for some of the incompatible element budget of clast D.

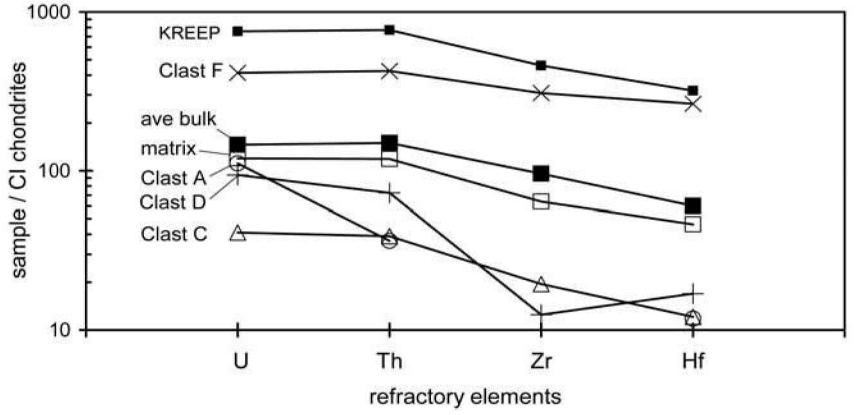

Fig. 5. Refractory element abundances of Calcalong Creek relative to CI chondrites. Calcalong Creek materials (bulk, matrix, clasts) all exhibit a decreasing trend that suggests that they are of dominant highland affinity. Clast D's pattern may be affected by slight matrix contamination.

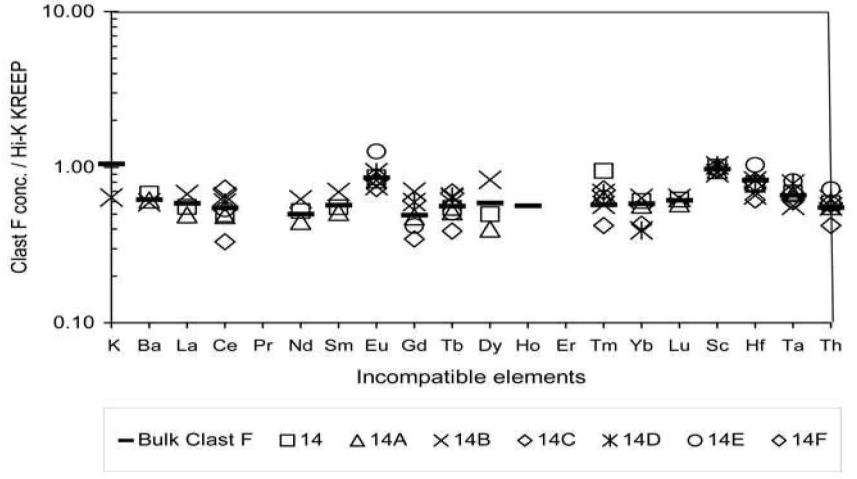

Fig. 6. Incompatible element abundances relative to CI chondrites for separated grains of clast F analyzed by INAA. While there are small differences between grains, they do not indicate significant heterogeneity of incompatible elements on a sub-mm scale (for clast F). The small differences are attributed to the distribution of Ce-bearing (REE-bearing) phosphate laths and needles <20 microns long (see Fig. 1h).

Table 5. Concentrations of Clast F grains counted separately late in the high flux INAA experiment.[a]

	14		14A		14B		14C		14D		14E		14F			
	1.013 mg	s.d.	0.872 mg	s.d.	0.19 mg	s.d.	0.398 mg	s.d.	0.16 mg	s.d.	0.142 mg	s.d.	0.173 mg	s.d.	ave .of grains	average all clast F
Na	6620	240	–	–	5760	60	–	–	–	–	–	–	–	–	5800	6780
Mg	–	–	–	–	–	–	–	–	–	–	–	–	–	–	–	3.2
Al	–	–	–	–	–	–	–	–	–	–	–	–	–	–	–	7.59
K	–	–	–	–	–	–	–	–	–	–	–	–	–	–	–	7230
Ca	8.43	0.27	8.6	0.3	7.2	0.4	–	–	–	–	–	–	–	–	8.2	8.25
Sc	23.12	0.25	21.96	0.22	21.00	0.21	22.00	0.29	23.6	0.24	22.4	0.4	22.6	0.4	22.3	22.4
Ti	–	–	–	–	–	–	–	–	–	–	–	–	–	–	–	11800
V	–	–	–	–	–	–	–	–	–	–	–	–	–	–	–	49
Cr	1535	17	1484	16	1319	17	1340	90	1427	19	1487	24	1531	23	1460	1463
Mn	–	–	–	–	–	–	–	–	–	–	–	–	–	–	–	1040
Fe	8.50	0.08	7.82	0.08	7.46	0.08	8.01	0.16	8.16	0.10	7.93	0.11	7.83	0.13	7.93	7.94
Co	19.67	0.28	18.32	0.20	17.98	0.20	20.07	0.22	17.06	0.20	17.16	0.21	16.72	0.18	17.95	17.95
Ni	230	50	120	18	237	7	n.d.	n.d.	217	17	n.d.	n.d.	n.d.	n.d.	221	221
Zn	23	17	7.3	1.5	4.5	0.4	n.d.	n.d.	4.5	0.9	n.d.	n.d.	n.d.	n.d.	4.68	4.7
Ga	14	4	–	–	–	–	–	–	–	–	–	–	–	–	14	14
Br	1.03	0.28	–	–	–	–	–	–	–	–	–	–	–	–	1.03	2.98
Rb	29.9	2.0	27.9	1.6	22.2	0.4	n.d.	n.d.	n.d.	n.d.	n.d.	n.d.	n.d.	n.d.	22.9	22.93
Sr	n.d.	n.d.	221	13	179	7	n.d.	n.d.	227	18	n.d.	n.d.	n.d.	n.d.	192	192
Zr	1320	50	1340	70	1229	17	853	25	1200	40	1270	130	950	110	1136	1135
Mo	5.1	0.5	–	–	2.2	0.4	–	–	–	–	–	–	–	–	3.44	3.4
Ag	–	–	–	–	2.5	0.5	–	–	–	–	–	–	–	–	2.5	2.5
Sb	0.089	0.024	n.d.	n.d.	0.088	0.023	n.d.	n.d.	n.d.	n.d.	n.d.	n.d.	n.d.	n.d.	0.09	n.d.
Cs	1.27	0.08	1.17	0.04	1.076	0.022	1.104	0.022	0.82	0.04	1.66	0.05	1.11	0.03	1.12	1.12
Ba	810	30	740	70	713	19	n.d.	n.d.	n.d.	n.d.	n.d.	n.d.	n.d.	n.d.	740	744
La	61.1	1.1	54.4	3.0	74.0	0.7	–	–	–	–	–	–	–	–	69.4	64.3
Ce	139.0	2.8	137.2	1.6	183.0	2.2	93	6	166.5	2.5	150	4	201	6	153	153
Nd	93	6	79.9	1.4	110.9	2.3	–	–	–	–	–	–	–	–	88.7	88.7
Sm	26.50	0.27	24.6	0.5	33.3	0.3	–	–	–	–	–	–	–	–	28.5	27.40
Eu	2.83	0.09	2.74	0.027	2.490	0.025	2.41	0.05	3.06	0.06	4.17	0.04	2.83	0.028	2.83	2.827
Gd	n.d.	n.d.	27.8	1.4	40.5	0.8	20.0	0.6	34.6	1.1	24.3	1.9	35.3	1.9	28.5	28.5
Tb	5.49	0.11	5.18	0.05	6.37	0.06	3.89	0.08	6.5	0.12	5.09	0.10	6.81	0.07	5.61	5.61
Dy	32.4	1.5	26	5	54	5	–	–	–	–	–	–	–	–	33.7	38.3
Ho	–	–	–	–	–	–	–	–	–	–	–	–	–	–	n.d.	7.9
Tm	5.4	0.4	3.58	0.10	3.27	0.06	2.41	0.07	3.9	0.08	3.65	0.23	4.06	0.25	3.27	3.27
Yb	21.8	0.4	20.55	0.23	22.88	0.25	15.5	0.5	14.1	1.4	–	–	–	–	20.9	20.9
Lu	3.10	0.03	2.91	0.029	3.18	0.03	n.d.	n.d.	n.d.	n.d.	n.d.	n.d.	n.d.	n.d.	3.05	3.06
Hf	30.0	0.3	29.6	0.3	25.00	0.25	23.40	0.12	31.20	0.22	39.2	0.4	30.5	0.3	31.4	31.34
Ta	3.4	0.1	3.38	0.07	2.83	0.06	2.99	0.15	3.92	0.04	4.06	0.04	3.09	0.03	3.3	3.30
W	–	–	–	–	4.20	0.08	–	–	–	–	–	–	–	–	4.2	2.3
Os	–	–	–	–	0.8	0.5	–	–	–	–	–	–	–	–	0.79	0.79
Ir	0.010	0.008	0.004	0.003	0.004	0.001	0.004	0.001	n.d.	n.d.	n.d.	n.d.	n.d.	n.d.	0.004	0.004
Au	0.011	0.003	–	–	0.003	0.001	–	–	–	–	–	–	–	–	0.004	0.005
Th	13.0	1.5	12.31	0.07	12.3	2.3	9.30	0.16	13.7	0.29	16	1	12.9	0.9	12.1	12.14
U	3.41	0.04	n.d.	n.d.	2.92	0.04	n.d.	n.d.	n.d.	n.d.	n.d.	n.d.	n.d.	n.d.	3.11	3.34

Table 5. Concentrations of Clast F grains counted separately late in the high flux INAA experiment.[a] *Continued.*

	14		14A		14B		14C		14D		14E		14F			
	1.013 mg	s.d.	0.872 mg	s.d.	0.19 mg	s.d.	0.398 mg	s.d.	0.16 mg	s.d.	0.142 mg	s.d.	0.173 mg	s.d.	ave .of grains	average all clast F
Oxide wt% calculated from INAA.																
SiO_2	–		–		–		–		–		–		–		–	54.48
TiO_2	–		–		–		–		–		–		–		–	1.97
Al_2O_3	–		–		–		–		–		–		–		–	14.34
FeO	10.94		10.06		9.60		10.31		10.50		10.21		10.08		10.20	10.77
MnO	–		–		–		–		–		–		–		–	0.13
MgO	–		–		–		–		–		–		–		–	5.31
CaO	11.79		12.03		10.07		n.d.		n.d.		n.d.		n.d.		11.53	11.54
Na_2O	0.89		–		0.78		–		–		–		–		0.78	0.91
K_2O	–		–		–		–		–		–		–		–	0.87
Cr_2O_3	0.22		0.22		0.19		0.20		0.21		0.22		0.22		0.21	0.21

[a]Table of concentrations of individual grains of clast F counted at late decay times in the high flux INAA experiment. The concentrations are in ppm except for Mg, Al, Ca, Fe, and K, which are in %. Two-sigma absolute uncertainties are listed next to each value. The blank entries indicate elements not processed for samples with late decays. The oxide wt% is calculated from the INAA determination.

Table 6. Concentrations of soils near Imbrium basin (PKT) and Calcalong Creek.[a]

				Calcalong Creek	
	Apollo 12	Apollo 14	Apollo 15	Ave. Bulk	Clast F
SiO_2	46.3	48.1	46.8	47.18	54.48
TiO_2	3.0	1.7	1.4	0.84	1.97
Al_2O_3	12.9	17.4	14.6	20.83	14.35
Cr_2O_3	0.34	0.23	0.36	0.17	0.21
FeO	15.1	10.4	14.3	9.69	10.22
MnO	0.22	0.14	0.19	0.14	0.13
MgO	9.3	9.4	11.5	7.11	5.31
CaO	10.7	10.7	10.8	13.31	11.50
Na_2O	0.54	0.7	0.39	0.49	0.91
K_2O	0.31	0.55	0.21	0.24	0.87
P_2O_3	0.40	0.51	0.18	0.1	n.d.
S	n.d.	n.d.	0.06	n.d.	n.d.
Total	99.1	99.8	100.8	100.09	99.95

[a]Apollo data from Basu and Riegsecker (1998). Calcalong Creek oxides were calculated from INAA data. P_2O_5 is based on an average of microprobe line scans.

comparisons, bulk samples and clast F follow a trend that includes the lunar meteorites Dhofar 25 and Dhofar 81. The trend is within a factor of 3 for Co/CI chondrites but spans almost an order of magnitude for Ni/Ir /CI chondrites (Fig. 7).

Overall, CI-chondrite normalized patterns of highly siderophile elements are similar for bulk samples of Calcalong Creek, QUE 94281, Y-793274, and to a lesser degree, EET 87521, suggesting that the class of impactor was probably the same at least for the predominant impact event (Fig. 8). However, there are enough distinguishing groupings on other elemental plots to indicate that the impactors were not of exactly the same composition. Clasts A and D display an excess Ir abundance. Possibly, all three meteorites were affected by a large basin impact whose imprint has been altered slightly by later impact gardening by projectiles of different compositions.

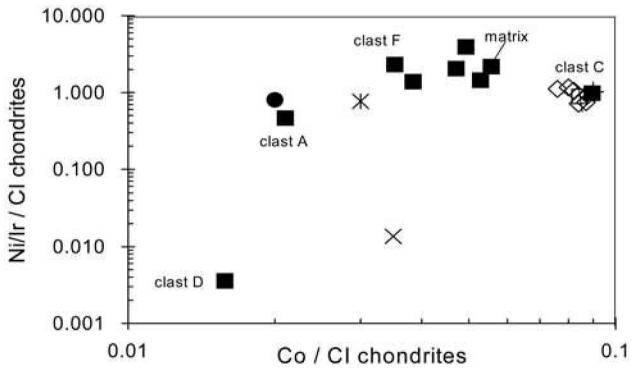

Fig. 7. Siderophile element comparisons for lunar meteorites for Co normalized to CI chondrites and Ni/Ir normalized to CI chondrites. Clast C and QUE 94281 may have impactors of similar composition, and/or the siderophiles of their source regions may be similar. The spread of Co values for Calcalong Creek samples may reflect indigenous differences in their source regions.

MINERALOGY AND "KREEPY" INCOMPATIBLE TRACE ELEMENTS

Calcalong Creek contains the highest abundance of incompatible elements of any lunar meteorite, most notably K, REE, and Th. Marvin and Holmberg (1992) found Calcalong Creek to be a mixture of welded, unrelated assemblages but no distinct KREEPy clasts or large, REE-bearing phosphates (whitlockite). They suggested that this small thin section was unrepresentative and/or the KREEPy carrier was in the melted matrix rather than in discrete clasts. We examined 2 more sections and also found no large phosphates or potassium-feldspar but, rather, small silica-rich clasts with and without K-feldspar and phosphates as bar-shaped grains or irregular grains in small clasts. One 200×400 micron clast contains both REE-rich and REE-poor phosphates <20 microns across and a La-enriched phase within a 50 micron vesicle (Fig. 9). Multiple microprobe line scans of Calcalong Creek average 0.10 wt% P_2O_5, typical of other lunar polymict breccias. Hence, possible REE carriers other than typical "KREEPy" materials may exist: REE may be in extremely tiny grains distributed throughout the matrix and/or in the glass that now welds the clasts. Some grains of armalcolite, tranquillityite, and Zr-containing silicates could have been original REE carriers. The matrix glass itself exhibits some heterogeneity with patches of mafic and anorthitic compositions. If the REE component is in the glass, it must be fairly well mixed; three bulk samples, a small matrix sample, and a clast-rich bulk sample all exhibit the same REE pattern and abundances. In addition, 3 of the 4 clasts studied by INAA exhibit the same pattern, although in differing abundances. This suggests that the KREEPy component may be in the melted matrix or the finest fraction grains, in addition to small phosphate-bearing and Zr-bearing clasts.

Clast F exhibits a relatively high incompatible element content that is unrelated to phosphate abundance (Ca), suggesting that there could be other, much smaller clasts or fragments of similar high-REE, Th, and U material. Matrix may have contaminated some of the surfaces of the clasts analyzed (Figs. 1d–1g). Alternatively, clasts may have mixed with matrix during shock melting. The KREEP component is ubiquitous in lunar samples and dominantly occurs as a cryptic contamination in breccias, as inferred by Ryder (1979). The similar incompatible element content in Calcalong Creek clasts and matrix could indicate an early chemical imprint.

We have addressed the possibility that the REE of Calcalong Creek may have been affected by terrestrial contamination. Although the vesicles present could provide a means for contamination as described by Crozaz and Wadhwa (2001), obvious weathering products, staining, or alteration were not observed (Marvin and Holmberg 1992). In addition, the REE patterns seen in Calcalong Creek do not exhibit any unusual LREE excess that would be attributable to contamination by Australian soils (Taylor and McLennan 1985; Swindle et al. 1998). The REE patterns measured by INAA are remarkably similar and, therefore, do not exhibit obvious contamination-related heterogeneities observed in other weathered meteorites from hot deserts (Crozaz and Wadhwa 2001). Key REE ratios (K/La, La/Sm, and Sm/Eu) are consistent with other basaltic lunar meteorites recovered in Antarctica and KREEP breccias and basalts recovered from the Apollo missions. Our conclusion is that there is minimal terrestrial REE contamination.

Microprobe analyses by Marvin (unpublished data) and our lab indicate that there is a predominance of high-Ca pyroxene grains and clasts in Calcalong Creek. Marvin suggested that the sample is, in general, an alkali anorthosite. These are common rocks and are generally restricted to the western lunar hemisphere. This is also consistent with the relative high abundance of incompatible elements, especially Th, that are found in the western region by remote sensing. The modes in alkali anorthosites range from nearly pure

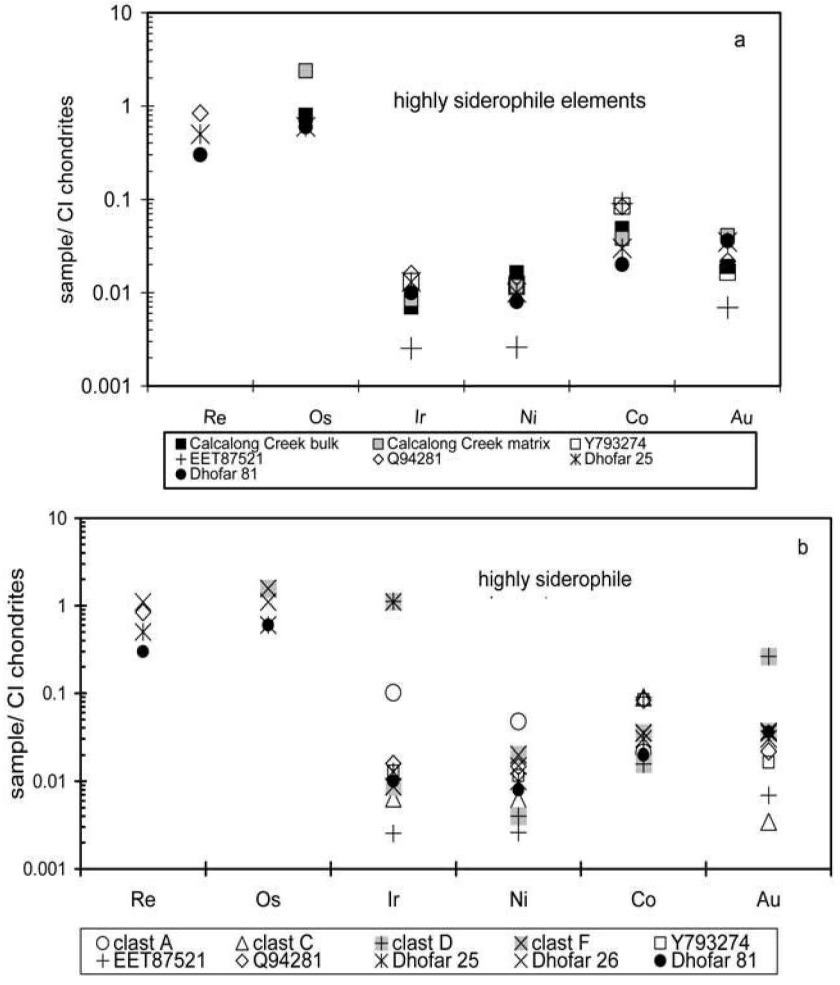

Fig. 8. Overall siderophile pattern of selected lunar meteorites. Considering their varied launch locations and times, they are remarkably similar: a) comparison of siderophile elements in bulk lunar meteorites to assess possible common impactors; b) comparison of siderophiles in Calcalong Creek clasts and other lunar meteorites.

anorthite to anorthitic norite in which there is ~84% plagioclase and 16% pyroxene with no olivine (Papike et al. 2000). Lack of equilibrium suggests rapid cooling and a possible shallow origin. Alkali anorthosites rarely exhibit the KREEP pattern or high K_2O of other evolved rocks (Papike et al. 2000). Calcalong Creek, while exhibiting some characteristics of alkali anorthosites, shares characteristics with mafic alkali rocks (7–25% Al_2O_3 and 4–16% MgO). Snyder and Taylor (1995) have suggested their origin as a cumulate from successive residual liquids that crystallized after alkali anorthosites. Shervais and McGee (1997) concluded that most mafic alkalis crystallized from magmas with REE similar to high-K KREEP.

The REE abundance pattern of the bulk Calcalong Creek meteorite could be dominated by incompatible-rich clasts and "contamination" of the matrix by melting. Or, the pattern could be carried in the smallest grain fraction of the matrix or as partially melted clasts. Other than clast F, we have not seen large, KREE-dominated clasts and, yet, 3 small but representative bulk samples yield very similar REE abundances. Most likely, the REE carrier has been incorporated into the matrix and fused into melt clasts. Phosphates, especially whitlockite, and K-feldspar in which the REE would normally reside are rare, so we looked for other carriers of the REE, K, and Th in the bulk samples. The REE pattern and abundances compared to some Apollo 15 "LKFM" basalts, along with many major element correlations, indicate some relationship to Apollo 15 materials (Table 6). The phosphorus content of Calcalong Creek is consistent with the bulk abundance of other polymict breccias that also contain a cryptic, KREEPy component. Bulk samples, glassy matrix, and even separated clasts all exhibit a KREEP-like REE pattern, suggesting that important carriers are in the finest fraction of grains and/or incorporated into the glassy matrix and fused into other unrelated clasts during lithification. Davis et al. (2001) reported on REE-bearing phosphate grains in vugs of 2 lunar crystalline impact melt breccias (76015 and 76215). They suggested that these were

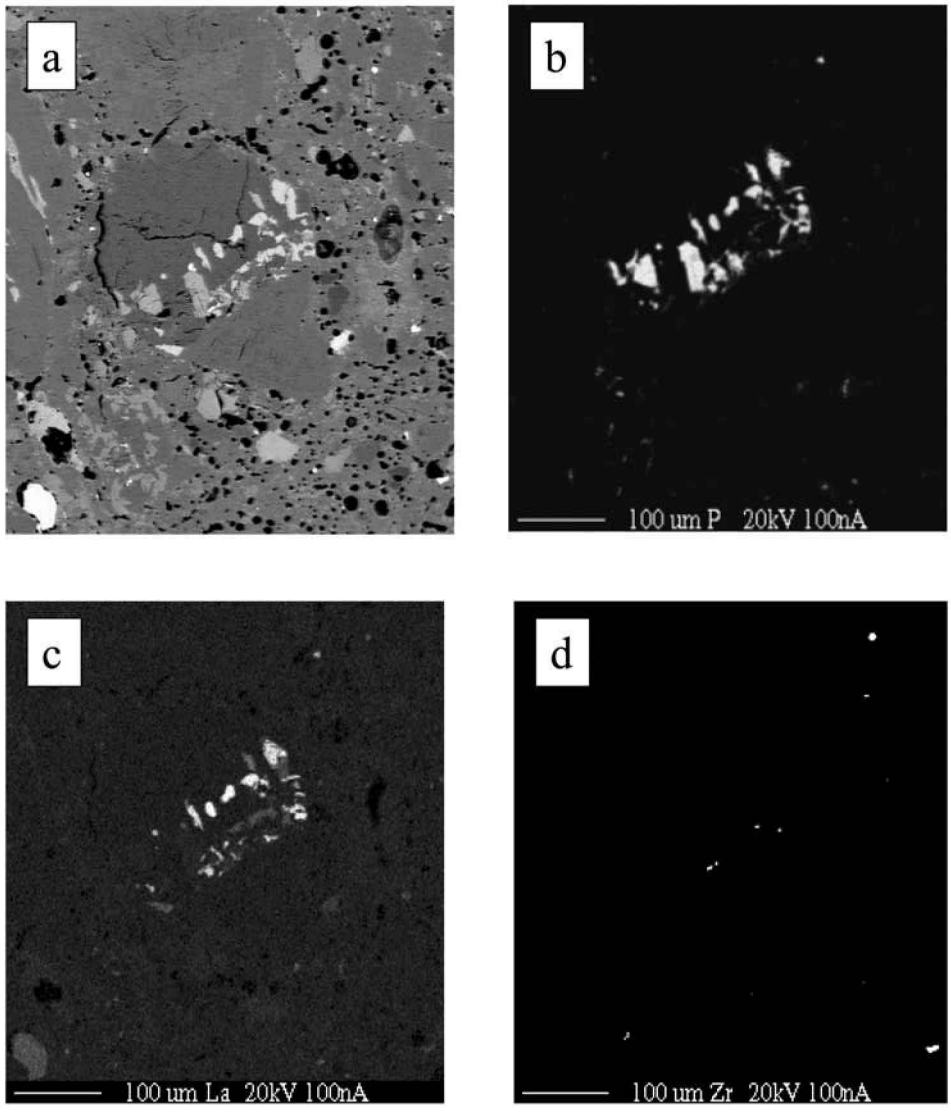

Fig. 9. Small, egg-shaped clast that contains a band of both REE-bearing and REE-poor phosphates. Its dimensions are ~ 200×400 microns. Other similar clasts may be important carriers of the REE in Calcalong Creek in addition to what is present in the melted matrix: a) BSE image of clast and surrounding matrix providing an X-ray view in which brighter regions are minerals with higher overall atomic numbers. The bright and light gray grains in the interior are phosphate minerals. The dark gray is plagioclase, and the medium gray is pyroxene; b) X-ray map of phosphorus minerals (mostly whitlockite) in the clast. The bright phases contain the most phosphorus. Not all of the P-rich minerals are REE-rich (see Fig. 9c); c) X-ray map of lanthanum in the clast. The brighter areas indicate higher concentrations of La and associated rare earth elements. The bright, La-bearing, 50 micron grain to the lower left is not associated with either phosphorus or zirconium bearing minerals; d) X-ray map of zirconium in the clast. In this clast and surrounding matrix, there is little correlation between the few high Zr bright spots and La (REE) often associated with Zr-bearing minerals.

deposited by a fluid phase based on the observed zoning trends. Calcalong Creek contains smaller, rounded phosphate grains at the edges of some vesicles that could also carry REE.

CLAST F AND KREEP TYPES

The INAA analyses displayed KREEPy chemical characteristics as defined by Snyder and Taylor (1995): K >2400 ppm (F = 7200 ppm) and La >28 ppm (F = 64 ppm). The Taylor et al. (1978) criteria would classify clast F as an LT basalt with CaO/Al_2O_3 = 0.80 and TiO_2 = 2%. They cautioned that "some VLT basalt lithic fragments may have compositions that do not reflect the composition of a genuine lunar magma." Furthermore, clast F would be considered a "med-K KREEP" clast, as outlined by Taylor et al. (1991), according to its K, La, and Lu abundances (Fig. 4). Taylor et al. (1991) also stated that "all known pristine KREEP rocks are med-K KREEP" and that ". . . components (of low-K

KREEP) could easily result from impact-induced mixing of med-K KREEP or hi-K KREEP with typical non-KREEPy highland rocks;" ". . . samples of low-K KREEP have been found as polymict breccias. . . ." We do not propose that clast F is pristine in the sense of a primary crystallization product. This clast, more likely, has undergone either assimilation of KREEPy material by mare basalt, assimilation of VLT/LT mare basalt by a KREEPy magma (Finnila et al. 1994), or impact mixing and partial melting of "previously" separated crystallization products. Clast F contains the chemical signature for KREEP for REE, K, Hf, Ta, and Th but is highly depleted in phosphorus. We note that while many authors have identified "KREEPy" materials, they usually report only major elements and trace elements easily analyzed by INAA: K, REE, and Th, omitting phosphorus (not determined by INAA). Possibly, some samples previously identified as "KREEPy" are really KREE-rich or, more precisely, incompatible rich. Korotev (1998, 2000) has recommended use of the term "incompatible-element rich mafic impact melt breccias," which we agree is more appropriate. As suggested earlier for the whole rock, the incompatible elements may be associated with mafic minerals but are below electron microprobe detection limits for spot analyses. Microprobe inspection of the INAA grains reveal minor grain to grain differences in phosphate abundances. The initial microprobe split may, in fact, contain fewer phosphates than the INAA grains.

Clast F's KREE(P) component could be related to the "same" KREEP layer (or composition) that underlies both the Apollo 15 and Luna 16 sites because it is similar to Apollo 15 KREEP in composition, but major elements are more closely associated with VLT mare basalt and Luna 16 alkaline basalts. Or, it may sample material from the "great lunar hot spot" that has since been identified with high Th abundances believed to indicate the presence of KREEP-rich material. This anomalously Th-rich region has been proposed to be the source of all KREEP-derived materials on the lunar surface. Calcalong Creek, clast F in particular, likely represents yet another variant of this KREEP-derived material.

COMPARISON WITH OTHER LUNAR METEORITES

VLT and LT Mare Basalt Sources in Common with Basaltic Lunar Meteorites

The mixed mare basalts and highlands materials in Calcalong Creek are most closely associated with those of other basaltic breccias: EET 87521, Y-793274, and QUE 94281 (Fig. 10). Arai et al. (1996) determined that the VLT mare basalt source for QUE 94281 pyroxenes contained bulk rock TiO_2 = 0.8%. They cited this as additional evidence for a "strong similarity" to Y-793274 (TiO_2 = 0.63%) and EET 87521 (TiO_2 = 1.1%). Interestingly, bulk Calcalong Creek has a similar TiO_2 abundance of 0.86%. However, Lindstrom et al. (1991, 1994) noted that the mare component of Y-793274 is of a magnesian VLT-type, similar to Apollo 17 VLT and that EET 87521 has a ferroan VLT composition like Luna 24 VLT. Both QUE 94281 and components of Calcalong Creek are generally more magnesian than Y-793274 and do not follow correlation trends of Luna 24 VLT basalts (Taylor et al. 1978). In addition, Calcalong Creek (particularly clast F) has higher alkali abundances with respect to both Apollo 17 VLT and Luna 24 VLT. We conclude that the mare basalt sources for Calcalong Creek are related to VLT basalts but not the same as the Apollo 17 or Luna 24 types. Its Ti content is high enough to be considered low-Ti or at the upper range of VLT. Bulk samples and clasts (except clast F?) also are not consistent with interelement trends of Fe versus Al_2O_3, MgO, or Cr_2O_3 for Apollo 17 and Luna 24 VLTs. One bulk split and clast F plot near "metabasalts" defined by MgO versus Cr_2O_3 (Ryder and Marvin 1978). Ryder and Marvin (1978) recognized that Luna 16 VLT basalts are more alkaline than Luna 24 VLT. Marvin and Holmberg (1992) described several clasts and assemblages of Calcalong Creek that are unusual mixtures most closely resembling Luna 24 and Luna 16 basalts but were found in association with "unrelated" late-stage crystallization products. They concluded that the "associations" were forced by possible impact melting and mixing.

Calcalong Creek is related to the VLT basalts found in other lunar meteorites, especially EET 87521, Y-793274, and QUE 94281. It is related to common crustal plagioclase sources as well. However, there are sufficient differences to indicate that the plagioclase source was not exactly the same. Warren and Kallemeyn (1993) investigated possible K assimilation in mare basalts from granitic rocks by comparing bulk rock K versus La. The predominantly mare lunar meteorite, EET 87521, and the predominantly highlands lunar meteorite, QUE 94281, both plot on the line defined by KREEP ratios (and most likely controlled by the small KREEP component). Y-793274, along with bulk and clast samples of Calcalong Creek, also plot parallel to the KREEP line but to the high-K side (Fig. 11). Clast F follows this trend but has high enough K to overlap the upper range of Apollo 14 VHK basalts that Warren and Kallemeyn (1993) suggest is the result of assimilation of granite. Other comparisons of Calcalong Creek samples also indicate potassium excess compared to typical KREEPy materials

Associated lunar meteorites with Mg-VLT affinities were plotted for Ni (compatible) and Zr (incompatible) along with other mare glasses (Fig. 12). Y-793274 and QUE 94281 plot near the lower end of the field that includes high-Ti Apollo 15 glasses, even though they are VLT-LT with respect to Ti (Shearer et al. 1996). Bulk samples of Calcalong Creek plot to the upper right (higher Zr and Ni) and are basically parallel to the Apollo 15 VLT field. The enriched Zr constituent is probably associated with the, so far, unidentified "incompatible-rich" phase, which is also the carrier of the

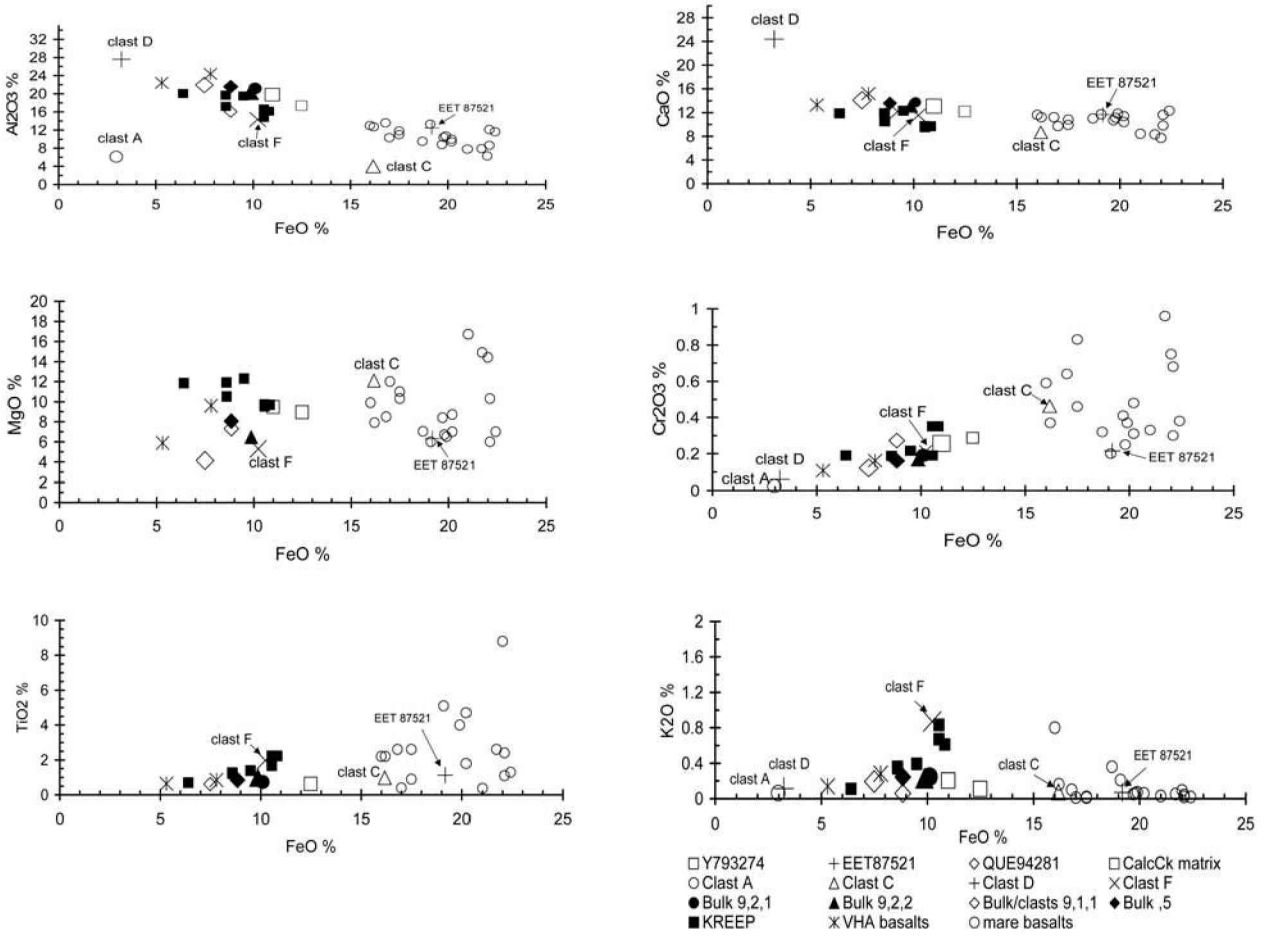

Fig. 10. Major element and oxide relationships between Calcalong Creek, related lunar meteorites, and other lunar materials. They reflect the trends and degree of fractionation of the source material.

REE. Small amounts of zirconium-bearing minerals have been observed in the matrix. Low-Ti glasses (Apollo and Luna) form a very different trend with much lower Zr and increasing Ni as well as a positive slope.

Rb/Sr Source Composition of Related Lunar Meteorites and Other Lunar Basalts

Rb is a highly incompatible element in magmatic melts, while Sr is less incompatible and tends to partition into plagioclase. Rb and Sr, therefore, concentrate in crustal materials and residua. The ratio can provide insight into differentiated products from a given source region. Shih (1975) suggested that since igneous processes tend to increase Rb/Sr in the melt, the Rb/Sr ratio for basalts can be considered to be the upper limit for their sources. Neal et al. (1994) also used Rb/Sr as an indicator of source composition or degree of partial melting. Bulk, matrix/agglutinate, and clast samples of Calcalong Creek exhibit particularly high ratios of Rb/Sr compared to low-Ti basalts. They range from 0.015 (clast D) to 0.12 (clast F) and a bulk ratio of ~0.07. The lowest ratio measured is higher than the upper range for low-Ti basalts (Shih 1975). The typical Rb/Sr ratio for VLT basalt is 0.014; for LT basalt is 0.01; for HT basalt is 0.003–0.038; and for Apollo 15 KREEP is 0.04–0.11. On this basis, Calcalong Creek's mare basalt component may originate from a source different from those found at Apollo or Luna sites, or it may be related to LT or VLT basalts that experienced a high degree of partial melting. The related lunar meteorites EET 87521 and QUE 94281 (Arai et al. 1996; Lindstrom et al. 1996) have Rb/Sr ratios which are also much higher than low-Ti mare basalts: 0.038 and 0.053, respectively (Warren and Kallemeyn 1989; this lab). Bulk and matrix samples of Y-793274 actually fall inside both the low-Ti and high-Ti basalt ranges with Rb/Sr ratios of 0.004 and 0.01 (Lindstrom et al. 1991). These 4 meteorites may represent varying degrees of partial melting of the same mare source.

Highlands Provenance and Plagiophile Elements

Warren (1986) studied "plagiophile" elements of lunar rocks in an effort to explain their bimodal distribution with

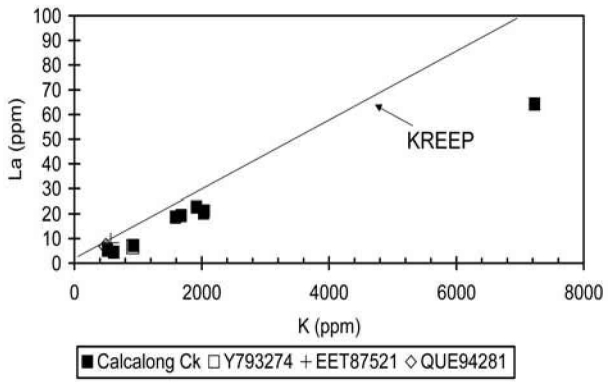

Fig. 11. K versus La for Calcalong Creek and other lunar samples. The strong lunar correlation is exhibited along with an enrichment of evolved incompatible elements.

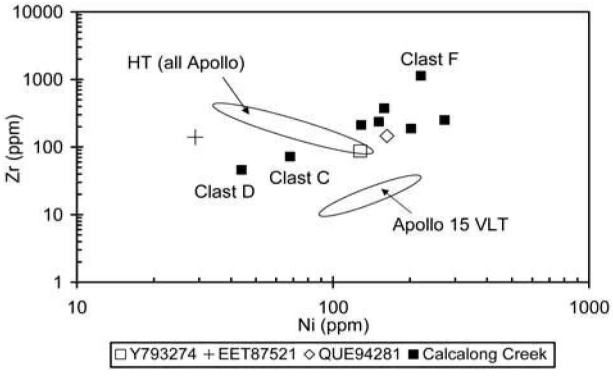

Fig. 12. Ni versus Zr. Comparison of VLT mare basalts in Calcalong Creek. Apollo 15 VLT and high-Ti fields are from Shearer et al. (1996).

respect to mg# (molar MgO/[MgO + FeO]). Comagmatic trends were identified as those with inverse correlations. Plots of mg# versus Eu/Al, Ga/Al, and molar Na/(Na + Ca) show that the bulk samples of EET 87521, QUE 94281, Y-793274, and Calcalong Creek form trends, suggesting that, at least, the plagioclase source was the same (Fig. 13). The Ga/Al ratio seems to display the greatest variation. All 4 meteorites appear in the same order on each plot (EET 87521 with the highest degree of fractional crystallization and Calcalong Creek with the smallest). The Eu/Al trend falls between the KREEP and ferroan anorthite fields. The Ga/Al trend is similar to and overlaps the lower "boundary" of the alkali anorthosites. However, the Na/(Na + Ca) trend lies in the middle of the ferroan anorthosite field, which exhibits a fairly "constant" Na/(Na + Ca) ratio over a large mg# range. Clast F is consistently high in plagiophile elements and plots near the KREEP and alkali anorthosite field. It is not collinear with the bulk lunar meteorites. Clast C is also an outlier: grouped with the lunar meteorites mentioned above for Eu/Al; higher than clast F for both mg# and Ga/Al, causing it to plot far outside the alkali anorthosite field; and low Na/(Na + Ca), which is far below the ferroan anorthosite field. Although the bulk meteorite samples generally exhibit a trend, clast F and clast C cannot have the same anorthite source provenance using this colinearity criterion. Sample ,9,1 contains more clasts than the other bulk samples. It has an mg# = 0.50, which is closest to that of clast F (0.48), but its plagiophile ratios are more similar to the bulk rock. This is consistent with the trend of other bulk, basaltic, lunar meteorites. This, too, indicates that clast F did not necessarily share the same plagioclase source. Clasts A and D exhibit similar but somewhat lower plagiophile element ratios.

IS CALCALONG CREEK FROM A PREVIOUSLY UNSAMPLED REGION?

Calcalong Creek was launched from a previously unsampled region of the moon. But, the chemistry of this region is related to VLT source regions and KREEP (also VHA and nonmare basalts) materials also sampled by the basaltic lunar meteorites and Apollo and Luna missions. The bulk composition of Calcalong Creek follows the trend that mare basalt clasts and components in all lunar meteorites are of the low-titanium (LT) or very low-Ti (VLT) varieties (Lindstrom et al. 1991; Warren and Kallemeyn 1991) (Fig. 14). This is in contrast to the abundant high-Ti (HT) mare basalts sampled and mapped by gamma-ray spectrometry by the Apollo missions (Metzger et al. 1979) and ground-based reflectance spectroscopy (Pieters 1978). Only a few of the basalts on the near side have been sampled (Pieters 1978) and, as we know that lunar meteorites are more random, representative samples of the moon, LT, and VLT mare basalts may be more abundant than previously thought (Warren and Kallemeyn 1991).

Initial mixing calculations for Calcalong Creek were consistent with a mixture of 50% anorthosite, 20% KREEP, 15% Luna 16 type LT mare basalt due to enriched alkalis and 15% SCCRV (Sc-Cr-V) components (Hill et al. 1991). In light of our final data, we concur with Korotev's (1999) mixing model: Calcalong Creek contains about 50% feldspathic material, 25% KREEP-norite, 25% VLT mare basalt, and 1% CI chondrite compositions. Korotev (1999) also required other, more specific but unknown components to account for "excess" elements such as Sc, Cr, and V. Indeed, Ryder (1979) noted that it is a common problem that KREEP-rich rocks are not modeled exactly by known pristine rocks or the observed clasts in the rock itself. Korotev (2000) also described this problem with regard to mixing models for mafic impact breccias.

Aluminum enrichment, low titanium, and other major element comparisons in Calcalong Creek reveal a strong association to the VHA basalts (group 1) of Dickinson et al. (1985). The La/Yb ratio ~2 for the bulk samples and clast F are also consistent with a VHA/KREEP basalt association (Hubbard and Rhodes 1977). Warren and Kallemeyn (1991) and others suggested that the "dichotomy between mare and nonmare products" might not be as well defined or as distinct

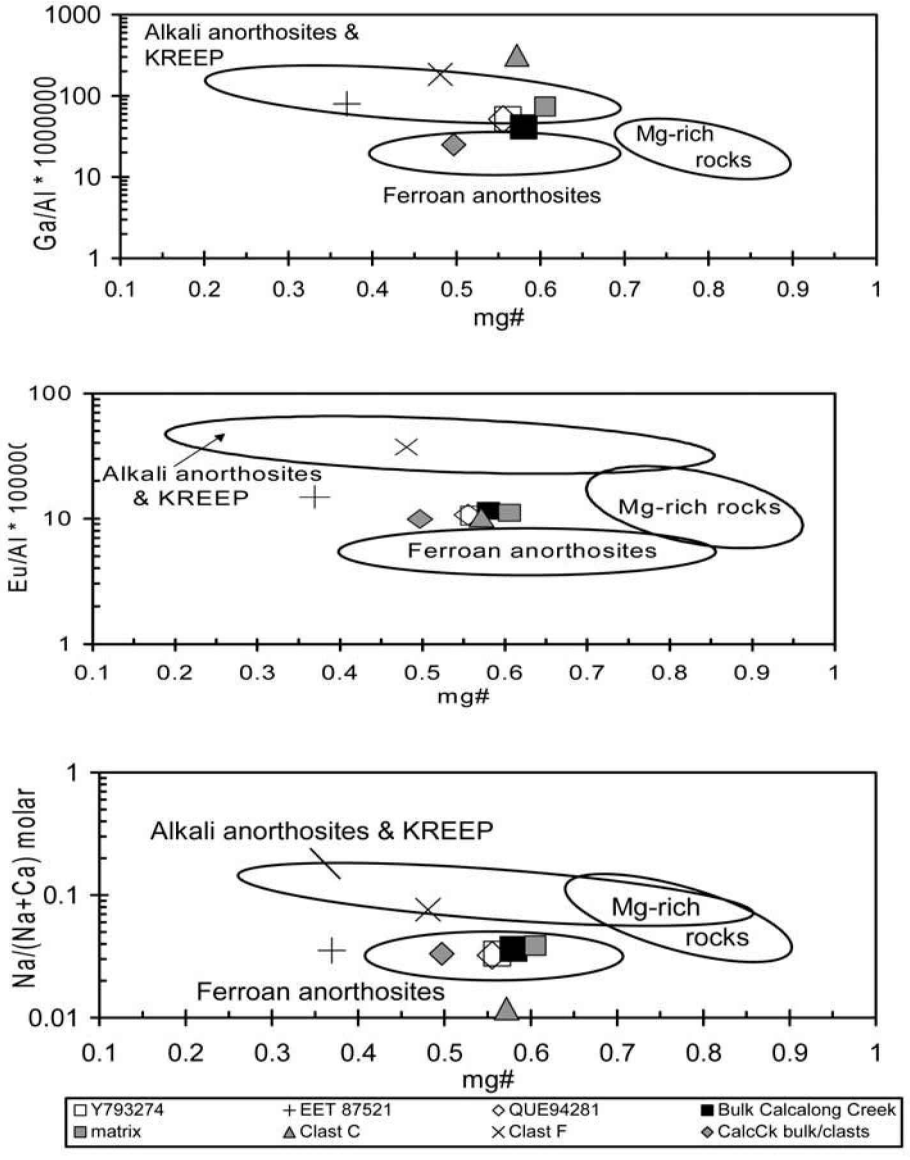

Fig. 13. Plagiophile element ratios indicate similar source regions for the anorthite component of basaltic lunar meteorite breccias. Clast F contains plagiophiles consistent with those from alkali anorthosites and KREEP source region. The diagram is after Warren (1986).

as once thought. Inconsistencies between major element compositions and trace element relationships of some unusual basaltic clasts have been explained by Shervais et al. (1985) to be hybrid magmas formed as mare basalts that assimilated aluminous KREEP basalts during their ascent. Alternatively, Ryder et al. (1977) proposed a "spectrum of source regions" for some aluminous basalt rock types transitional to mare and KREEP basalts. In addition, there seems to be significant variation in the major element compositions of samples identified as "KREEPy." Because Calcalong Creek may sample new basalt types, what appears to be VLT in affinity is also possibly a new low-titanium highland basalt hybrid or new rock type.

Taylor and Bence (1975) noticed decreasing abundances compared to CI chondrites of the refractory elements U, Th, Zr, and Hf for highlands crust and especially KREEPy samples. An increasing trend was seen for mare basalts. Calcalong Creek materials (bulk, matrix, clasts) all exhibit a decreasing trend that suggests they are of dominantly highlands provenance (Fig. 5). Although their absolute abundances vary by an order of magnitude, all of the samples except two clasts (A and D) display parallel patterns. Most likely, this is due to varying amounts of highlands crust that were incorporated into each or, alternatively, differences in their source regions or both. Bulk and matrix abundances are almost midway between those of clasts F and C, the highest and lowest measured respectively. Clasts A and D, while exhibiting a decreasing trend of these refractory elements,

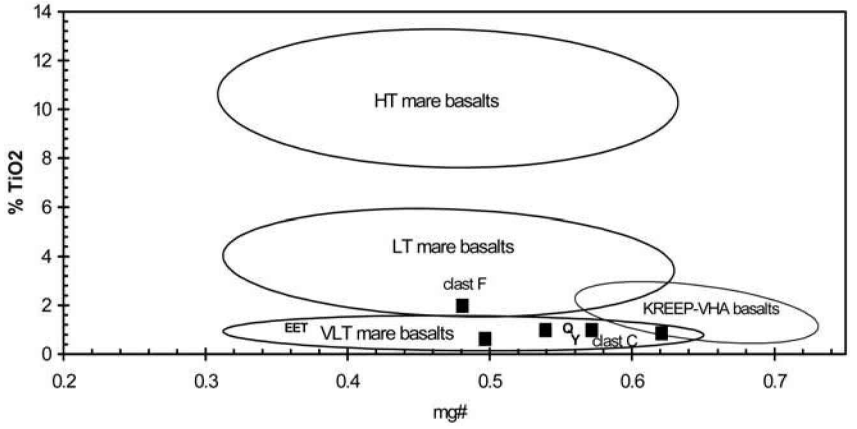

Fig. 14. Comparison of mg# and TiO_2 of the mare basalt component in Calcalong Creek compared to other basaltic lunar meteorites, high-Ti mare basalts (HT), low-Ti mare basalts (LT), and very low-Ti mare basalts (VLT). Bulk INAA samples exhibit an affinity for VLT basalts, while clast F is more similar to LT basalts. The reference fields are from BVSP.

deviate from the predominant pattern. Clast A displays a large U excess by about 3× what would be suggested by its Th and Hf contents (which are the same as clast C) (Fig. 5). However, this U excess is not significant at the 2-sigma uncertainty of its measurement. Clast D also displays possible slight U excess and contains a much lower relative abundance of Zr. Representative KREEP and mare basalts do not exhibit this marked Zr depletion. The low-Ti mare basalt 14053 exhibits a smaller depletion of Zr but also has much less Hf than clast D; their patterns are not similar. We suggest that clasts A and D are probably exotic inclusions that were incorporated into the breccia. The highlands-like pattern displayed by Clast C, VLT mare basalt, is most likely due to its incorporation of highlands material during impact mixing.

POSSIBLE LAUNCH SITES AND PROVENANCE OF CALCALONG CREEK

Numerous telescopic observations and lunar spacecraft missions (Apollo, Galileo, Clementine, and Lunar Prospector) have allowed identification of mare basalt types within mare regions based on TiO_2 content. Pieters and McCord (1975) categorized the following maria as VLT basalts with <1.5% TiO_2: Late Imbrium-Schickard, Frigorus C, E Sinus Roris, Sominorium, Imbrium (?), Nubium (?), and Procellarum (?). LT mare basalts (1.5–2% TiO_2) were found in the Apollo 15 region (Le Monier, Plato, west edge of Serenitatis), Imbrium (?), and Humorum (?). More recently, Lucey et al. (1996) mapped global FeO and TiO_2 concentrations with low-resolution Clementine images of the South Pole-Aitken basin (SPA). They found that the floor of SPA is "unlike any major lunar or model lunar mantle composition" and suggest that it is a 1:1 mixture of LKFM mafic impact melts and lunar mantle compositions. Alternatively, they propose that it could be a mixture of average highlands norites and troctolites with low-Ti mare basalts or lower crustal impact melts similar in origin to LKFM but with lower TiO_2 and Th. The ~10–16% FeO, <2% TiO_2, and 2–4 ppm Th abundances reported for SPAT exhibit remarkable similarity to bulk Calcalong Creek (9.7, 0.8, 4.3, respectively) (Table 7). Lunar Prospector data, however, suggest that KREEP materials in the SPA basin are in low abundance. Calcalong Creek displays bulk and clast TiO_2 (0.8%) abundances and mineralogy suggestive of VLT affinity (Marvin and Holmberg 1992) but also includes a clast ("F") with nearly 2% TiO_2, indicating more of an LT affinity for that clast. While bulk Calcalong Creek may appear to contain similar abundances of FeO, TiO_2, and Th to SPA, we will argue that the main material actually has stronger connections to PKT.

What Lunar Regions Are Represented?

The provenance of Calcalong Creek is most likely near the PKT as suggested by Korotev et al. (1999). Our sampling of clasts indicates that it is a mixture of both mare and highland components. Its high Th and K abundances indicate that it could have come from a region consistent with a lunar near side, western highlands composition. The clast population in Calcalong Creek represents the local well-mixed highland regolith from this launch site (Fig. 3). Some clasts, such as clast F, and the matrix that welded the sample are related to materials from the Imbrium basin impact that excavated the PKT. We can relate the compositions only in a chemical sense, since they have been altered and mixed by multiple impact processes. Based on our trace-element studies, we suggest that Calcalong Creek is a sample of the regolith of a mare/highlands boundary region (Fig. 15). This carried the chemical overprint of the Procellarum Imbrium basin-forming event that ejected REE-rich and Th-rich material. The predominant signature of the highlands materials is related to the feldspathic region that has been

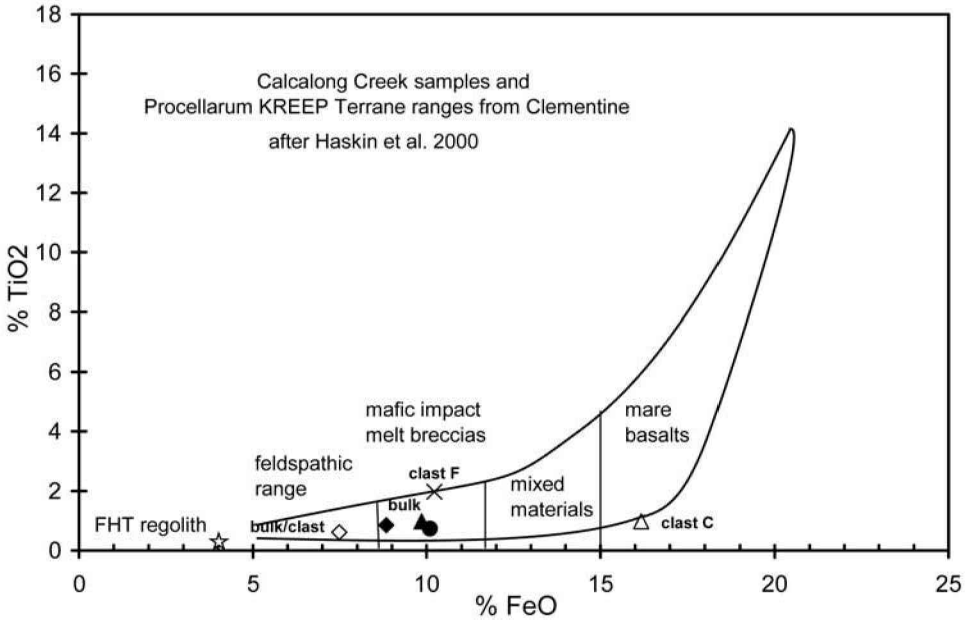

Fig. 15. This figure illustrates an alternative interpretation that Calcalong Creek bulk and INAA clast compositions are consistent with a wholly near side origin in the PKT and FHT with mixing of nearby mare basalts through large basin-forming impact (Imbrium bolide) and smaller multiple impacts. This is in contrast to the suggestion that it has incorporated "exotic" far side SPAT material.

identified as the FHT by Jolliff et al. (2000) and others. Clast A may have experienced mixing with the postulated Imbrium ejecta as evidenced by its KREE (P) patterns and abundances, Th, and FeO relationships. Clast D, while of predominant highlands or FHT affinity, contains enough thorium to have come from either the FHT or SPAT according to the Th-distance correlation by Haskin et al. (2000) (Fig. 17). However, major element correlations, refractory elements, and others preclude a direct connection to SPAT. Clast D, more likely, represents FHT ~1000–1500 km from the center of the Imbrium basin.

Clast C is of mare affinity with some similarities to SPAT composition except for possible excess FeO (Table 7). As might be expected, it contains an abundance of Th that corresponds to a range of distance from the Imbrium basin of 2000 km up to that of the SPAT (~4500 km). Even though diagrams by Haskin et al. (1999, 2000) illustrate relationships of "non-mare" samples, they provide insight into other lunar samples as well. The FeO and TiO_2 content in clast C are also consistent with the composition of mare basalts found within the PKT (Fig. 15). This could also be coincidental. Although Calcalong Creek is related to materials in the western near side, Imbrium ejecta in particular, clast C could have been ejected from the far side as there is some similarity of the mafic component to the SPAT. The planned sample return mission from SPA will provide a more comprehensive composition for comparison.

Using Clementine spacecraft gamma-ray data, Jolliff et al. (2000) addressed the question of the source of Th enrichment. Is it due to basaltic volcanism or impact excavation of a deeper KREEP-rich layer in the upper crust? They studied the distribution of Th-rich materials as a function of elevation within and near the PKT and found that most, but not all, of the higher elevation regions were also higher in Th. The volcanically resurfaced areas and the "rugged terrain" were both found to contain about 5–6 ppm Th. Jolliff et al. (2000) proposed that these were mare basalts (and not KREEP basalts) due to their high FeO concentrations. Calcalong Creek bulk samples (including matrix) contain 3.4–4.4 ppm Th, which is only slightly lower than this region. Its FeO content, however, is more consistent with a KREEP-like source. The mare clast C is more similar to typical (VLT) mare basalts with a Th concentration of 1.1 ppm and 16.2% FeO. Clast F contains 12.1 ppm Th and 10.2% FeO, which is almost the same abundance as "endogenous KREEP" basalt found at the Apollo 15 site (Warren and Wasson 1979) and is also thought to underlie the PKT and many of the Apollo and Luna sites. The Th and FeO of bulk samples of Calcalong Creek fall within the range of the PKT (Fig. 16). Calcalong Creek possibly contains samples postulated by Jolliff et al. (2000), as small clasts and mixed matrix, to be derived from sub-Imbrium crust as evidenced by the high-Th content of clast F. This is probably the relatively high-Th and REE carrier seen throughout the rock. If part of Calcalong Creek did sample the PKT, as Korotev and others suggest, it may add credence to the idea that a large region of the moon experienced widespread KREEP basaltic volcanism of the Apollo 15 type in the lower crust before the formation of the Procellarum and Imbrium basins and that additional basin-filling basalts were induced

Table 7. Three geologic terranes of the lunar crust and the Calcalong Creek lunar meteorite.[a]

	FeO wt%	TiO2 wt%	Th ppm
Feldspathic Highlands Terrane (FHT)			
(Anorthositic)	4.2 (0.5)	–	0.8 (0.3)
Basin ejecta-covered	5.5 (1.6)	–	1.5 (0.8)
Calcalong Creek clast A	2.97 (0.07)	n.d.	1.04 (0.22)
Clast D	3.23 (0.28)	n.d	2.07 (0.04)
Procellarum KREEP Terrane (PKT)			
(Mare)	15–20	<1–15	3–7
Calcalong Creek clast C	16.2 (0.14)	0.98 (0.18)	1.12 (0.02)
(Nonmare)	9.0 (1.6)	–	2–6; 5.2 (1.4)
Mixed	10.7 (2.6)	–	4.5 (2.0)
Calcalong Creek clast F	10.22 (0.04)	1.97 (0.10)	12.14 (0.08)
Bulk	8.84–10.10 (0.07)	0.73–0.98 (0.1)	3.76–4.40 (0.08)
Matrix	10.98 (0.12)	n.d.	3.39 (0.03)
South Pole-Aitken Terrane (SPAT)	10–16%	<2	2–4
(Inner)	10.1 (2.1)	–	1.9 (0.4)
(Outer)	5.7 (1.1)	–	1.0 (0.3)
Calcalong Creek clast C	16.2 (0.14)	0.98 (0.18)	1.12 (0.02)

[a]The lunar terrane data are from Lucey et al. (1996), Jolliff et al. (2000), and Haskin et al. (2000). Absolute uncertainties are listed next to each value. For bulk samples of Calcalong Creek, the highest uncertainty measured is listed. Clast C is listed twice for ease of comparison with mare and SPAT.

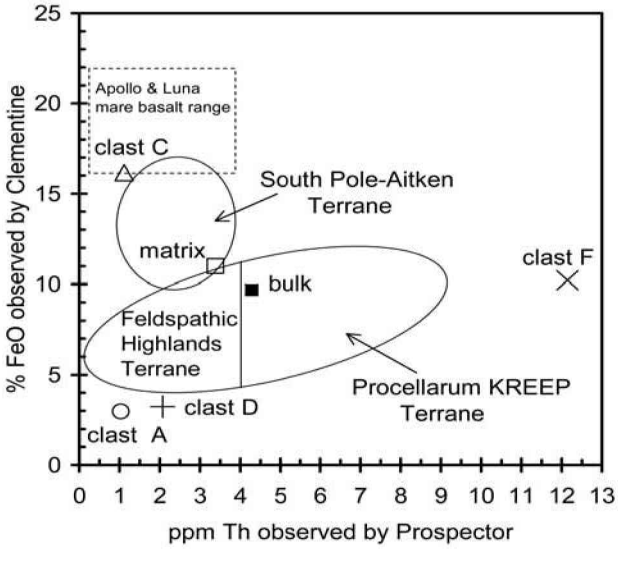

Fig. 16. Comparison of Th and FeO in Calcalong Creek materials as they relate to lunar terranes identified from Lunar Prospector and Clementine data. Diagram is based on Jolliff et al. (2000). Plots of Th, FeO, and TiO_2 data from remote spacecraft data and analyses of lunar samples returned from known locations (Apollo and Luna programs) result in the same terrane assignments and associated distances.

by the impact. Slight volatile enrichment on grains and scarce meteoritic metal does tend to favor some kind of exposure to volcanic processes. ZnS, FeS, and other sulfur-enriched grains were found to be associated with vesicles and matrix. From our data, we are unable to confirm or refute Gillis and Jolliff's (1999) contention that the KREEPy material observed on a moon-wide scale is solely from mare volcanism. They identified 9 craters in or near the PKT with high Th abundances and only the largest, Plato (101 km diameter), exhibits low Th and FeO similar to bulk Calcalong Creek and clast F.

Composition and Distance from Imbrium Basin

Alternatively, Haskin et al. (1999) proposed that the provenance of most of the feldspathic materials in Th-rich mafic impact melt breccias found at Apollo sites, except Apollo 17, are "the substrates onto which molten Imbrium ejecta fell," now referred to as FHT. As evidence, they cite the common nature of the KREEPy melt component (mg# ~0.61), and ubiquitous incompatible trace elements similar to the Apollo 15 KREEP basalt. We note that Calcalong Creek is consistent in this regard; the matrix and bulk samples exhibit an mg# range of 0.54 to 0.62. Interestingly enough, clast F displays the lowest measured mg# of 0.48. Haskin et al. (1999) propose a process that might explain some of the exotic materials as well as the matrix of Calcalong Creek: molten Imbrium ejecta containing upper crustal (feldspathic) material dissolved in the ejecta would be transported some distance and descend as melt at high velocity onto sites of secondary cratering. Haskin et al. (1999) suggeted that part or most of the clastic feldspathic material of mafic impact melt breccias would be incorporated at the site of the secondary impact. This is consistent with the chemistry and texture of Calcalong Creek.

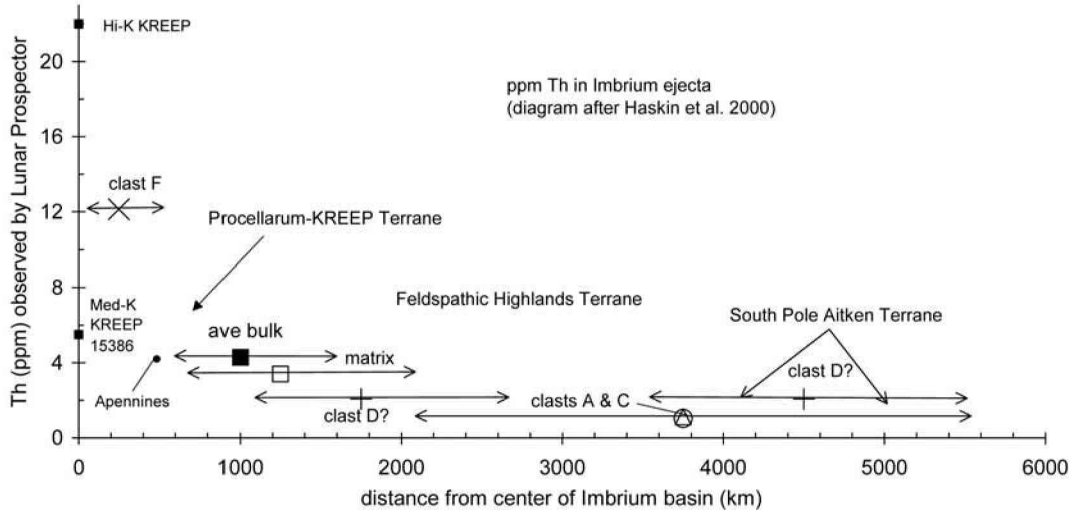

Fig. 17. Relationship of Calcalong Creek materials to their possible provenance, illustrating the amount of Imbrium ejecta that may be included in Calcalong Creek clasts, matrix, and bulk samples based on Th content only. Haskin (1998) found a correlation between distance from the Imbrium basin and Th content for both lunar samples returned by the Apollo missions and remote observations by Lunar Prospector. All 3 terranes may be represented in Calcalong Creek clasts: PKT, FHT, SPAT. The diagram reference is drawn after Haskin (1998).

The feldspathic component of Calcalong Creek does not "match" any particular Apollo regolith. It is most similar to Apollo 16 soils but is enriched in alkalis. Haskin et al. (1999) also remarked that ". . . agglutinates and glass spheres would be uncommon . . . because they would have dissolved or become too diluted by excavation and mixing of material of the megaregolith. . . ." Indeed, we do not see glass spheres and few, if any, agglutinates in Calcalong Creek. Furthermore, Vaniman and Papike (1980) modeled the radial distance traveled by the turbulent surge and found that it may be as much as one crater diameter in distance. Haskin (1998) studied the Th abundances at various distances from the PKT and associated Imbrium basin and found a clear correlation in the Apollo samples. As remarked by Korotev (1999), Calcalong Creek, as the lunar meteorite with the highest Th content, is most closely related to the PKT. According to the Haskin model, the matrix and bulk samples correspond to an ejecta distance of approximately <1000 km from the center of the Imbrium basin and >70% primary material (Fig. 17). Calcalong Creek's Th content (4.28 ppm) is remarkably close to the data reported for the Apollo 15 Apennines (Th ~4.6 ppm; <1000 km), already noted as the most similar of the Apollo KREEPy materials to Calcalong Creek. From Haskin's correlation, clasts A, C, and D may have a provenance corresponding to an ejecta distance of ~1000–3000 km (near side) or 4000–5500 km (far side) (Fig. 17). Or, they may have been "contaminated" through subsequent impact mixing with material of higher Th concentration from the PKT that formed the matrix. Clast F, a mixture of LT mare basalt material and REE-rich highland component with an even higher abundance of Th (12 ppm), has a stronger relationship to the PKT and is associated with an ejecta deposit distance extrapolated to the interior of the Imbrium basin itself (Haskin 1998). Individual grains of clast F reveal a range of Th from 9.3 ppm to 15.9 ppm. This could be a sample of assimilated LT mare basalt and KREEPy materials studied by Shervais et al. (1985) that survived the large impact event. Some authors have referred to the existence of both "plutonic" KREEPy materials as well as KREEPy volcanism that was induced by a large impact from which all of the incompatible-rich rocks are derived. While the markers for Imbrium ejecta on the lunar surface are high Th and "KREEP-related" elements originating from the "high-Th oval" or "great lunar hot spot," Haskin (2000) noted the presence of Th in some maria. Heat flow measurements confirm the presence of a global, K-U-Th-enriched layer beneath the surface (Haskin 2000). Recent studies suggest that this layer is probably not continuous as well as heterogeneous. Ryder et al. (1997) have proposed that the KREEP target was at or near the liquidus at the time of impact because few pristine KREEP clasts are observed in the lunar rocks. Several workers have suggested that the impact of a large bolide into a partially molten, heterogeneous (KREEP-rich) target (Haskin 2000; Korotev 2000; and others) would result in the observed variations of alkali anorthosite and incompatible elements derived from the "Th hot spot" (PKT) and found in breccias with different proportions of mantle and feldspathic upper crust. We believe these ideas are all consistent with the observations of Calcalong Creek clasts, matrix, and chemical components.

CONCLUSION

The incompatible elements in Calcalong Creek, while associated with the Apollo 15 "LKFM" basalt source, represent yet another variant of heterogeneous KREEP-derived material widely found on the moon. Calcalong Creek is related to the LT and VLT materials found in other lunar

meteorites, but it is not from the same source. Calcalong Creek, along with the other lunar meteorites, demonstrates that most of the mare basalts must be LT and VLT. The mare component of Calcalong Creek, clast C in particular, appears to have an affinity for materials in the SPAT as well, which suggests that it may represent basalts not sampled previously. Plots of Th, FeO, and TiO_2 data from remote spacecraft and analyses of lunar samples returned from known locations (Apollo and Luna programs) result in the same terrane assignments and associated distances for Calcalong Creek. The major, minor, and trace-element compositions of Calcalong Creek provide evidence of mixing of the PKT, FHT, and possibly, SPAT-type material by multiple impact processes, the largest of which was the Imbrium bolide. Clearly, Calcalong Creek shares the complexity and diversity of materials that are found throughout the moon. While not necessarily a unique solution to the data, this is the first step toward relating Calcalong Creek to its lunar setting.

Acknowledgments–We wish to thank Harry Doane, Wayne Lohmeier, and Robert Offerle of the University of Arizona TRIGA reactor, the University of Arizona's Radiation Control Office for their ever-ready accommodation, and the University of Missouri personnel for their services. We thank Tom Teska and, especially, Ken Domanik for his expert assistance and dedication to the Lunar & Planetary Laboratory's Cameca electron microprobe lab, and Edgar Chavez (Cameca) for his ever-attentive service. We thank Michael Thompson for his assistance with the rabbit irradiations. As always, we appreciate the care with which David Mann made the superb thin sections. We thank Ursula Marvin and Beth Holmberg for their participation in this study and access to their data. Alex Ruzicka, Paul Warren, and Randy Korotev provided stimulating discussions on all things lunar. Richard Hill, Anna Spitz, Alan Hildebrand, and Charlene Carmony provided much appreciated encouragement. We thank Robert A. Haag for his generous donation of the sample. We appreciate the reviewers' comments, which significantly improved the manuscript. This work was conducted under NASA grant # NAGW 3373 to W. V. Boynton.

Editorial Handling—Dr. Urs Krähenbühl

REFERENCES

Basaltic Volcanism Study Project (BVSP). 1981. *Basaltic volcanism on the terrestrial planets.* New York: Pergamon Press. 1286 p.

Basu. A. and Riegsecker S. 1998. In *Workshop on new views of the Moon: Integrated remotely sensed, geophysical, and sample datasets*, LPI Contribution No. 958, edited by Jolliff B. L. and Ryder G. Houston: Lunar and Planetary Institute. pp. 20–21.

Crozaz G. and Wadhwa M. 2001. The terrestrial contamination of Saharan shergottites Dar al Gani 476 and 489: A case study of weathering in a hot desert environment. *Geochimica et Cosmochimica Acta* 65:971–978.

Davis A. M., Dufek J. D., and Wadhwa M. 2001. Euhedral phosphate grains in vugs and vesicles in ordinary meteorites, lunar samples and the Ibitira eucrite: Implications for trace element transport processes. *Meteoritics & Planetary Science* 36:A47.

Delaney J. S. 1989. Lunar basalt breccia identified among Antarctic meteorites. *Nature* 342:889–890.

Delano J. W. 1986. Pristine lunar glasses: Criteria, data, and implications. Proceedings, 16th Lunar and Planetary Science Conference. *Journal of Geophysical Research* 91:D201–213.

Dickinson T., Taylor J. G., Keil K., Schmitt R. A., Hughes S. S., and Smith M. R. 1985. Apollo 14 aluminous mare basalts and their possible relationship to KREEP. Proceedings, 15th Lunar and Planetary Science Conference. *Journal of Geophysical Research* 90:C365–C374.

Finnila A. B., Hess P. C., and Rutherford M. J. 1994. Assimilation by lunar mare basalts: Melting of crustal material and dissolution of anorthite. *Journal of Geophysical Research* 99: 14677–14690.

Gillis J. J. and Jolliff B. L. 1999. Lateral and vertical heterogeneity of thorium in the Procellarum KREEP terrane; as reflected in the ejecta deposits of post-Imbrium craters. In *Workshop on new views of the moon II: Understanding the moon through the integration of diverse datasets*, LPI Contribution No. 980, edited by Gaddis L. and Shearer C. K. Houston: Lunar and Planetary Institute. pp. 18–19.

Haskin L. A. 1998. The Imbrium impact event and the thorium distribution at the lunar highlands surface. *Journal of Geophysical Research* 103:1679–1689.

Haskin L. A. and Warren P. H. 1991. Lunar chemistry. In *Lunar sourcebook, A user's guide to the moon*, edited by Heiken G., Vaniman D., and French B. New York: Cambridge University Press. pp.357–474.

Haskin L. A., Gillis J. J., Jolliff B. L., and Korotev R. L. 1999a. On the distribution of Th in lunar surface materials (abstract #1858). 30th Lunar and Planetary Science Conference. CD-ROM.

Haskin L. A., Korotev R. L., and Jolliff B. L. 1999b. Clast provenance in Imbrium impact-melt breccias (abstract #1942). 30th Lunar and Planetary Science Conference. CD-ROM.

Haskin L. A., Gillis J. J., Korotev R. L., and Jolliff B. L. 2000. The nature of mare basalts in the Procellarum KREEP terrane (abstract #1661). 31st Lunar and Planetary Science Conference. CD-ROM.

Hawke B. R. and Head J. W. 1979. Impact melt volumes associated with lunar craters (abstract). 10th Lunar and Planetary Science Conference. pp. 510–512.

Hill D. H., Boynton W. V., and Haag R. A. 1991. A lunar meteorite found outside the Antarctic. *Nature* 352:614–617.

Hill D. H., Marvin U. B., and Boynton W. V. 1995. Clasts from the Calcalong Creek lunar meteorite (abstract). 26th Lunar and Planetary Science Conference. pp. 605–606.

Hörz F. and Cintala M. J. 1997. Impact experiments related to the evolution of planetary regoliths. *Meteoritics & Planetary Science* 32:174–209.

Hubbard N. J. and Rhodes J. M. 1977. A chemical model for lunar non-mare rocks. In *Soviet-American conference on cosmochemistry of the moon and planets*, edited by Pomeroy J. H. and Hubbard H. J. Washington D.C.: NASA, U.S. Government Printing Office. pp. 137–151.

James O. 1996. Siderophile elements in lunar impact melts define nature of the impactors (abstract). 27th Lunar and Planetary Science Conference. pp. 603–604.

Jolliff B. L. 1999. Large-scale separation of K-frac and REEP-frac in the source regions of Apollo impact melt breccias, and a revised estimate of the KREEP composition. In *Planetary petrology and geochemistry, The Lawrence A. Taylor 60th birthday volume*,

edited by Snyder G. A., Neal C. R., and Ernst W. G. Columbia: Bellwether Publishing, Ltd. pp.135-154.

Jolliff B. L., Gillis J. J., Haskin L. A., Korotev R. L., and Wieczorek M. A. 2000.. Major lunar crustal terranes: Surface expressions and crustal-mantle origins. *Journal of Geophysical Research* 105:4197–4216.

Jolliff B. L., Gillis J. J., Haskin L. A., Korotev R. L., and Wieczorek M. A. 1999. Major lunar crustal terranes: Surface expressions and crust-mantle origins (abstract #1670). 30th Lunar and Planetary Science Conference. CD-ROM.

Jolliff B. L. and Haskin L. A. 1998. Integrated studies of impact-basin ejecta as probes of the lunar crust: Imbrium and serenitatis. In *Workshop on new views of the moon: Integrated remotely sensed, geophysical, and sample datasets*, LPI Contribution No. 958, edited by Jolliff B. L. and Ryder G. Houston: Lunar and Planetary Institute. pp. 43–44.

Korotev R. L. 1999. Lunar meteorites and implications for compositional remote sensing of the lunar surface. In *New views of the moon II: Understanding the moon rhrough the integration of diverse datasets*, LPI Contribution 980, edited by Gaddis L. and Shearer C. K. Houston: Lunar and Planetary Institute. pp. 36–38.

Korotev R. L. 1999. The great lunar hot spot and the composition and origin of LKFM impact-melt breccias (abstract #1305). 30th Lunar and Planetary Science Conference. CD-ROM.

Korotev R. L. 2000. The great lunar hot spot and the composition and origin of the Apollo mafic ("LKFM") impact-melt breccias. *Journal of Geophysical Research* 105:4317–4345.

Laul J. C., Morgan J. W., Ganapathy R., and Anders E. 1971. Meteoritic material in lunar samples. Proceedings, 2nd Lunar and Planetary Science Conference. *Geochimica et Cosmochimica Acta* 2:1139–1158.

Laul J. C., Rode O. D., Simon S. B., and Papike J. J. 1987. The lunar regolith: Chemistry and petrology of Luna 24 grain size fractions. *Geochimica et Cosmochimica Acta* 51:661–673.

Lindstrom D. J., Wentworth S. J., Martinez R. R., and McKay D. S. 1994. Trace element identification of three chemically distinct very low titanium (VLT) basalt glasses from Apollo 17. *Geochimica et Cosmochimica Acta* 58:1367–1375.

Lindstrom M. M., Mittlefehldt D. W., Martinez R. R., Lipschutz M. E., and Wang M. S. 1991. Geochemistry of Yamato-82192, -86032, and -793274 lunar meteorites. *Proceedings of the NIPR Symposium on Antarctic Meteorites* 4:12–32.

Lucey P. G., Taylor J. G., Hawke B. R. 1996. FeO and TiO_2 concentrations in the South Pole-Aitken basin: Implications for mantle composition and basin formation. *Journal of Geophysical Research* 103:3701–3708.

Marvin U. B. and Holmberg B. B. 1992. Highland and mare components in the Calcalong Creek lunar meteorite (abstract). 23rd Lunar and Planetary Science Conference. pp. 849–850.

Metzger A. E., Johnson T. V., and Matson D. L. 1979. A comparison of mare surface titanium concentrations obtained by spectral reflectance and gamma-ray spectroscopy: An early assessment. Proceedings, 10th Lunar and Planetary Science Conference. pp. 1719–1726.

Naney M. T. and Crowl D. M. 1976. The Apollo 16 drill core: Statistical analysis of glass chemistry and the characterization of a high-alumina silica-poor (HASP) glass. Proceedings, 7th Lunar and Planetary Science Conference. pp. 155–184.

Nishiizumi K., Arnold J. R., Caffee M. W., Finkel R. C., and Southon J. 1992. Exposure histories of Calcalong Creek and LEW 88516 meteorites (abstract). *Meteoritics* 27:270.

Nishiizumi K., Caffee M. W., Finkel R. C., and Reedy R. C. 1995. Exposure history of lunar meteorite QUE 93069 (abstract). 26th Lunar and Planetary Science Conference. pp. 1051–1052.

Ostertag R. D., Bischoff A., Palme H., Schultz L., Spettel B., Weber H., Weckwerth G., and Wanke H. 1986. Lunar meteorite Yamato-791197: Petrography, shock history, and chemical composition. *Proceedings of the 10th Symposium on Antarctic Meteorites*. pp. 17–44.

Palme H., Spettel B., Jochum K. P., Dreibus G., Weber H., Weckwerth G., Wanke H., Bischoff A., and Stöffler D. 1991. Lunar highland meteorites and the composition of the lunar crust. *Geochimica et Cosmochimica Acta* 55:3105–3122.

Papike J. J., Ryder G., and Shearer C. K. 2000. Lunar samples. In *Reviews in mineralogy 36: Planetary materials*, edited by Papike J. J. Washington D.C.: Mineralogical Society of America. pp. 1–234.

Pieters C. and McCord T. B. 1975. Classification and distribution of lunar basalt types. Proceedings, Conference on the Origin of Mare Basalts and Their Implications for Lunar Evolution. pp. 125–129.

Pieters C. M. 1978. Mare basalt types on the front side of the moon: A summary of spectral reflectance data. Proceedings, 9th Lunar and Planetary Science Conference. pp. 2825–2849.

Quick J. E., Albee A. L., Ma M. S., Murali A. V., and Schmitt R. A. 1977. Chemical compositions and possible immiscibility of two silicate melts in 12013. Proceedings, 8th Lunar and Planetary Science Conference. pp. 2153-2189.

Rhodes J. M. and Hubbard N. J. 1973. Chemistry, classification, and petrogenesis of Apollo 15 mare basalts. Proceedings, 4th Lunar and Planetary Science Conference. pp. 1127–1148.

Ryder G. 1979. The chemical components of highlands breccias. Proceedings, 10th Lunar and Planetary Science Conference. pp. 561–581.

Ryder G. and Stockstill K. R. 1997. Constituents of the lunar crust at the Serenitatis target: Least squares mixing calculations for Apollo 17 poikilitic impact melt rocks. Proceedings, 28th Lunar and Planetary Science Conference. pp. 1227–1228.

Ryder G., Stoeser D.B., and Wood J. A. 1977. Apollo 17 KREEPy basalt: A rock type intermediate between mare and KREEP basalts. *Earth and Planetary Science Letters* 35:1–13.

Ryder G. and Norman M. D. 1978. Catalog of pristine non-mare materials, Part 2. Anorthosites. JSC Publication No. 14603, Houston: NASA Johnson Space Center. 86 p.

Schaal R. B. and Hörz F. 1980. Experimental shock metamorphism of lunar soil. Proceedings, 11th Lunar and Planetary Science Conference. pp. 1679–1695.

Schaal R. B., Hörz F., Thompson T. D., and Bauer J. F. 1979. Shock metamorphism of granulated lunar basalt. Proceedings, 10th Lunar and Planetary Science Conference. pp. 2547–2571.

See T. H. F. and Cintala M. J. 2001. Experimentally produced shock melts in impact-comminuted powders of an L6 ordinary chondrite (abstract #1807). 32nd Lunar and Planetary Science Conference. CD-ROM.

Shearer C. K., Papike J. J., and Layne G. D. 1996. Deciphering basaltic magmatism on the moon from the compositional variations in the Apollo 15 very low-Ti picritic magmas. *Geochimica et Cosmochimica Acta* 60:509–528.

Shervais J. W., Taylor L. A., Lindstrom M. M. 1985. Apollo 14 mare basalts: Petrology and geochemistry of clasts from consortium breccia 14321. Proceedings, 15th Lunar and Planetary Science Conference. *Journal of Geophysical Research* 89:C375–C395.

Shervais J. W. and McGee P. E. 1997. KREEP in the western lunar highlands: An ion microprobe study of alkali and Mg-suite cumulates from the Apollo 12 and 14 sites (abstract). 28th Lunar and Planetary Science Conference. pp. 1301–1302.

Shih C. Y., Haskin L. A., Wiesmann H., Bansal B. M., and Brannon J. C. 1975. On the origin of high-Ti mare basalts. Proceedings, 6th Lunar and Planetary Science Conference. pp. 1255–1285.

Simon S. B., Papike J. J., Hörz F., and See T. H. 1986. An experimental investigation of agglutinate melting mechanisms: Shocked mixtures of Apollo 11 and 16 soils. Proceedings, 17th Lunar and Planetary Science Conference. *Journal of Geophysical Research* 91:E64–E74.

Simonds C. H., Warner J. L., Phinney W. C., and McGee P. E. 1976. Thermal model for impact breccia lithification: Manicouagan and the moon. Proceedings, 7th Lunar and Planetary Science Conference. pp. 2509–2528.

Snyder G. A. and Taylor L. A. 1995. Another sortie for pristine rocks at Mare Tranquillitatis: Chemistry of 1–4 mm basaltic fragments in soil 10085, 1161 (abstract). 26th Lunar and Planetary Science Conference. pp. 1327–1328.

Snyder G. A. and Taylor L. A. 1995. The growth and modification of lunar crust: KREEP basalt crystallization and precipitation of Mg- and alkali suite cumulates (abstract). 26th Lunar and Planetary Science Conference. pp. 1325–1326.

Stöffler D., Knoll H. D., Marvin U. B., Simonds C. H., and Warren P. H. 1980. Recommended classification and nomenclature of lunar highland rocks—A committee report. In *Proceedings of the conference on the lunar highlands crus*t, edited by Papike J. J. and Merrill R. B. New York: Pergamon Press. pp. 51–70

Swindle T. D., Burkland M. K., and Grier J. A. 1995. Noble gases in the lunar meteorites Calcalong Creek and Queen Alexandra Range 93069 (abstract). *Meteoritics* 30:584–585.

Swindle T. D., Kring D. A., Burkland M. K., Hill D. H., and Boynton W. V. 1998. Noble gases, bulk chemistry, and petrography of olivine-rich achondrites Eagles Nest and Lewis Cliff 88763: Comparison to brachinites. *Meteoritics & Planetary Science* 33: 31–48.

Taylor J. G., Warner R. D., and Keil K. 1978. VLT mare basalt: Impact mixing, parent magma types, and petrogenesis. In *Mare crisium: The view From Luna 24*, edited by Papike J. J. and Merrill R. B. New York: Pergamon Press. *Geochimica et Cosmochimica Acta* 9:357–370.

Taylor J. G., Warner R. D., Wentworth S., Keil K., and Sayed U. 1978. Luna 24 lithologies: Petrochemical relationships among lithic fragments, mineral fragments, and glasses. In *Mare crisium: The view from Luna 24*, edited by Papike J. J. and Merrill R. B. New York: Pergamon Press. *Geochimica et Cosmochimica Acta* 9: 303–320.

Taylor S. R. and Bence A. E. 1975. Trace elements characteristics of the mare basalt source region: Implications of the cumulate versus primitive source model. Proceedings, Conference on the origin of mare basalts and their implications for lunar evolution. Lunar Science Institute Contribution No. 234. pp. 159–163.

Taylor S. R. and McLennan S. M. 1985. *The Continental crust: Its composition and evolution.* Oxford: Blackwell Science Publishing. 312 p.

Vaniman D. T. and Papike J. J. 1980. Lunar highland melt rocks: Chemistry, petrology and silicate mineralogy. In *Proceedings of the conference on the lunar highlands crust*, edited by Papike J. J. and Merrill R. B. New York: Pergamon Press. *Geochimica et Cosmochimica Acta* 12:271–337.

Warren P. H. 1986. Anorthosite assimilation and the origin of the Mg/Fe-related bimodality of pristine moon rocks: Support for the magmasphere hypothesis. Proceedings, 16th Lunar and Planetary Science Conference. *Journal of Geophysical Research* 91:D331–343.

Warren P. H. and Kallemeyn G. W. 1989. Elephant Moraine 87521: The first lunar meteorite composed of predominantly mare material. *Geochimica et Cosmochimica Acta* 53:3323–3330.

Warren P. H. and Kallemeyn G. W. 1991. Geochemical investigation of five lunar meteorites: Implications for the composition, origin, and evolution of the lunar crust. *Proceedings of the NIPR Symposium on Antarctic Meteorites* 4:91–117.

Warren P. H and Kallemeyn G. W. 1993. Geochemical investigation of two lunar mare meteorites: Yamato-793169 and Asuka-881757. *Proceedings of the NIPR Symposium on Antarctic Meteorites* 6:35–57.

Warren P. H. and Wasson J. T. 1979. The origin of KREEP. *Reviews of Geophysics and Space Physics* 17:73–88.

Warren P. H, Jerde E. A., and Kallemeyn G. W. 1989. Lunar meteorites: Siderophile contents and implications for the composition and origin of the moon. *Earth and Planetary Science Letters* 91:245–260.

Warren P. H., Taylor L. A., Kallemeyn G. W., Cohen B. A., and Nazarov M. A. 2001. Bulk-compositional study of three Dhofar lunar meteorites: Enigmatic siderophile results for Dhofar 026 (abstract #2197). 32nd Lunar and Planetary Science Conference. CD-ROM.

Wieczorek M. A. and Phillips R. J. 1999. Thermal modeling of mare volcanism and the Procellarum KREEP terrane (abstract #1547). 30th Lunar and Planetary Science Conference. CD-ROM.

Wood J. A. 1975. Lunar petrogenesis in a well-stirred magma ocean. Proceedings, 6th Lunar and Planetary Science Conference. pp. 1087–1102.